Diamond on GaN for high power devices

Elena C. Persaud

2019

Supervisor: Professor Paul May
Second assessor: Dr Neil Fox

This thesis is submitted in partial fulfilment of the requirements for the Honours degree of Chemistry BSc at the University of Bristol

Elena C. Persaud

Acknowledgments

Elena C. Persaud

Abstract

This project involves the exploration of diamond growth by chemical vapour deposition (CVD) on gallium nitride (GaN) and contains two associated sections, a literature review and an experimental laboratory-based section. The literature review section discusses the use of diamond thin films grown by CVD, which provide thermal management for GaN high-power devices limited by overheating. The diamond layer permits the rapid conduction of localized heat in the GaN device towards a heat sink. Methods of resolving adhesion issues between diamond and GaN layers include the incorporation of an additional thin interfacial layer to relieve strain and enhance the close-packing of the layers.

The experimental laboratory-based section of this investigation explores the effect of incorporating an interfacial layer between GaN and diamond in order to improve adhesion at the interface between the layers.

Aluminium interlayers of the thickness range 1.5-40.3 nm were deposited onto the GaN surface, followed by mixed electrospray seeding and a 6-hour CVD diamond growth run using a microwave plasma-enhanced CVD reactor. A control sample without an Al interlayer was also prepared and used as a baseline for this investigation. The aim is to identify the thickness of interlayer that creates a strong chemical interface that can withstand compressive stress and ultimately prevent delamination of the deposited diamond layer. The samples produced were characterized by SEM and XRT imaging. Raman spectroscopy was also utilized to confirm the presence of sp^3 diamond deposited and to note the formation of graphitic carbon species during the CVD diamond growth. The samples containing 20.0 and 40.3 nm Al interlayers were characterized as most effective towards preventing diamond film delamination and improving the interfacial adhesion between GaN and diamond.

Elena C. Persaud

Table of Contents

Elena C. Persaud

1. Literature Review

Diamond on GaN for high power devices

1.1 Introduction to Diamond and GaN

Gallium nitride-based high-power electronic devices demonstrate the potential to operate efficiently at high power and high frequencies to outperform traditional Si-based devices in speed and electrical power. Promising GaN-based technologies include 5G base stations, satellites and radars [1]. However, GaN-based technology is limited by poor heat dissipation and overheating in the device. The heat build-up in the device can be minimized with the incorporation of a diamond layer that possesses exceptional thermal properties.

Widely recognized for its natural beauty, diamond is a metastable allotrope of carbon that has set itself apart due to its superlative properties, along with both promising and realised industrial applications. The stable lattice of diamond is solely comprised of singly bonded sp^3 hybridized carbon atoms arranged in an infinite repeating tetrahedral structure (Figure 1a)).
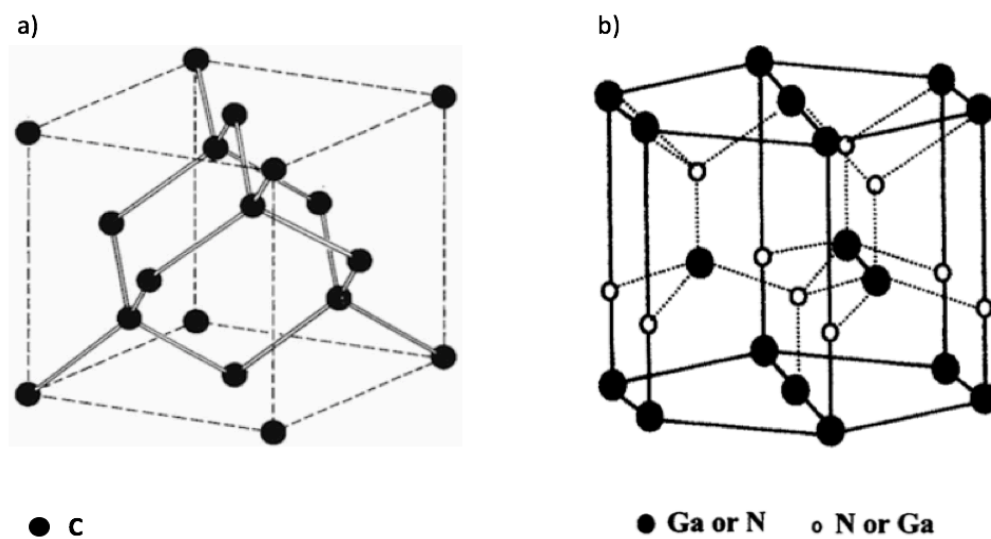
Figure 1. a) Face-centred cubic (FCC) crystal structure of diamond, noting the four single σ bonds formed by every sp^3 hybridized carbon atom b) Hexagonal close packed (HCP) wurtzite crystal structure of GaN, where every Ga is tetrahedrally bonded to four N atoms and *vice versa* [2] [3].

Although large scale production of high-quality diamond in a cost effective way still poses challenges, its unparalleled physical properties (Table 1) motivates scientists to devise new and improved methods of growing synthetic diamond for use in a commercial manner.

Elena C. Persaud

Over the past few years, group III-V semiconductors and specifically gallium nitride (GaN) has been the focus of research for the fabrication of high-power devices and optoelectronics. GaN crystals display the hexagonal wurtzite type structure, where every atom makes four covalent bonds in a tetrahedral manner (Figure 1b)). The substantial difference in electronegativity between Ga and N atoms makes the bonds partly ionic and hence very stable. GaN is a promising semiconductor with high electron mobility and a direct wide band gap (3.4 eV) due to strong chemical bonding. These properties combined with high chemical stability allow GaN devices to operate at high frequency and high voltage levels whilst minimizing leakage currents [4]. GaN displays astounding chemical, structural and electrical properties, however GaN-based devices suffer from overheating and malfunction due to its poor thermal properties. Diamond's superlative thermal properties, specifically its high thermal conductivity, permits GaN devices containing a polycrystalline diamond thin film to reach even higher power densities and frequencies.

Table 1. Physical properties of polycrystalline diamond and GaN for use in electronic applications.

	Polycrystalline Diamond	GaN	References
Hardness	80 GPa	10.2 GPa	[5], [6]
Melting Point	5000 K	2500 K	[7], [8]
Thermal Conductivity (300 K)	20 W cm^{-1} K^{-1}	1.3 W cm^{-1} K^{-1}	[9], [8]
Band Gap	5.45 eV	3.42 eV	[9], [8]
Specific Heat Capacity (300 K)	6.57 J mol^{-1} K^{-1}	35 J mol^{-1} K^{-1}	[10], [11]
Resistivity (300 K)	1.0×10^{12} Ω cm	1×10^{-1} Ω cm	[5], 12
Density	3.52×10^3 Kg m^{-3}	6.15×10^3 Kg m^{-3}	[13], [8]
Electron Mobility	2200 cm^2 V^{-1} s^{-1}	1000 cm^2 V^{-1} s^{-1}	[13], [8]
Thermal Expansion Coefficient (300 K)	1.0×10^{-6} K^{-1}	5.6×10^{-6} K^{-1}	[9], [8]
Thermal Expansion Coefficient Mismatch GaN	81.8%	0%	[9], [9]
Lattice constants	a= 3.57 Å	a= 3.19 Å c= 5.19 Å	[5], [8]
Lattice mismatch with GaN	89%	0%	[9], [9]

Naturally occurring diamonds are extremely expensive and scarce, as they are formed from carbonaceous deposits on average 100 miles below the Earth's surface, where conditions of high pressure and high temperature (HPHT) exist [14]. This natural process has been mimicked to make synthetic diamonds, however the process is expensive and limits the applications of the diamond. As such, another technique was developed to allow for more gentle growth conditions, higher quality diamonds and more diverse applications – chemical vapour deposition (CVD).

1.2 Chemical Vapour Deposition CVD

1.2.1 Chemical Vapour Deposition CVD: Introduction & Activation Types

In the 1970s a technique termed chemical vapour deposition (CVD) was developed to avoid the high pressure, high temperature conditions, allowing for the deposition of thin polycrystalline smooth diamond films of enhanced quality on various substrates. In this process a precursor molecule containing carbon is commonly diluted in excess hydrogen and activated. The original activation technique, hot filament CVD (HFCVD), is a thermal method of activating the CH_4/H_2 gases in the reactor using hot wires.

Microwave plasma assisted CVD (MWCVD) is a later-developed technique that utilizes microwaves to activate the gases in the chamber of a microwave plasma assisted CVD reactor (Figure 2). Carbon atoms are deposited at rates of typically 1-5 μm h^{-1}, yielding thin polycrystalline diamond layers on solid substrates [15]. One major issue holding back the large-scale production of CVD diamond is the necessity for an increase in diamond deposition rates to around 100-200 μm h^{-1} without a decrease in quality [16]. Also, achieving large area uniform growth is challenging in MWCVD as the plasma is spherical, thus a temperature gradient exists across the substrate.

An important advantage of MWCVD is that linearly ramping up the microwave power of the reactor results in a linear increase in the rate of diamond deposition, however operating at high powers is costly [17].
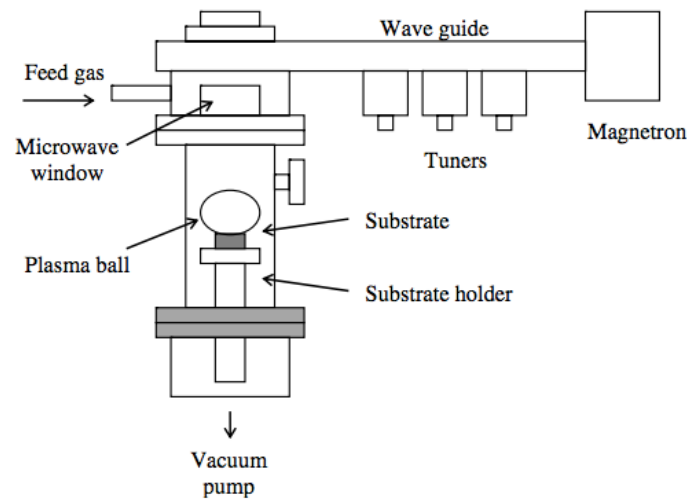
Figure 2. Diagram of microwave plasma assisted CVD reactor and apparatus [18].

1.2.2 Chemical Vapour Deposition Mechanism of Diamond Film Growth

The diamond CVD process involves the deposition of a solid layer onto a substrate, originating from reactants in the gaseous phase. Activated gas molecules, atoms and radicals take part in further complex reactions and finally diffuse towards the substrate surface. Subsequently, a suitable reaction site is located by the species and heterogeneous surface reactions under the required conditions result in the nucleation of the surface film, which constitutes a base additional growth (Figure 3). Finally, the homogenous growth and fusion of crystals allows the deposition of polycrystalline diamond film onto the surface.
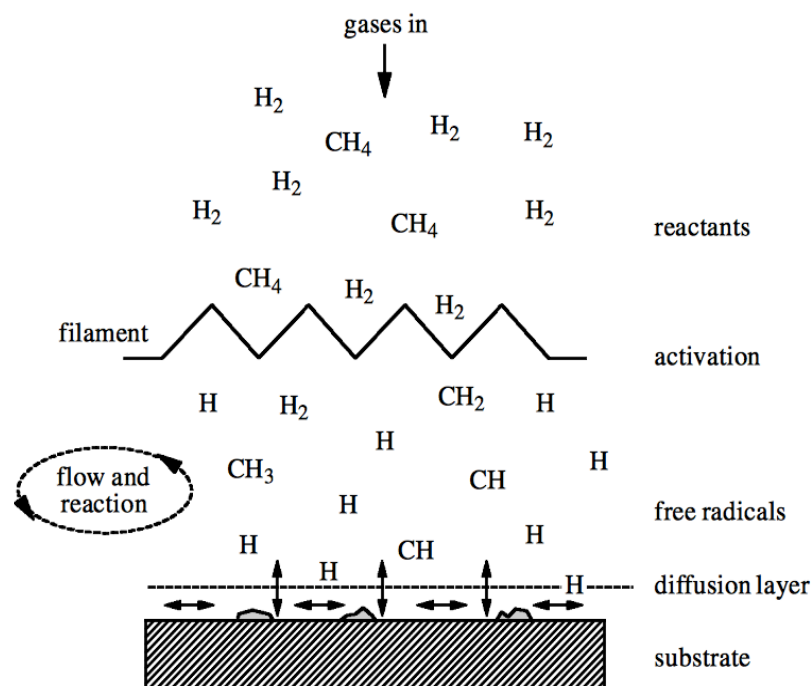
Figure 3. Diamond CVD deposition scheme of chemical and physical processes [19].

It is essential to understand that diamond deposition takes place at a region of specific gas composition, regardless of the gas mixture or deposition process. The ideal gas composition is illuminated in a C-H-O diagram; the 'Bachmann triangle diagram'. Diamond growth is identified in the defined dark grey region over the CO tie-line (Figure 4). The chemical processes are driven by H atoms that are formed by H_2 dissociation and therefore should be in high concentration in the chamber.
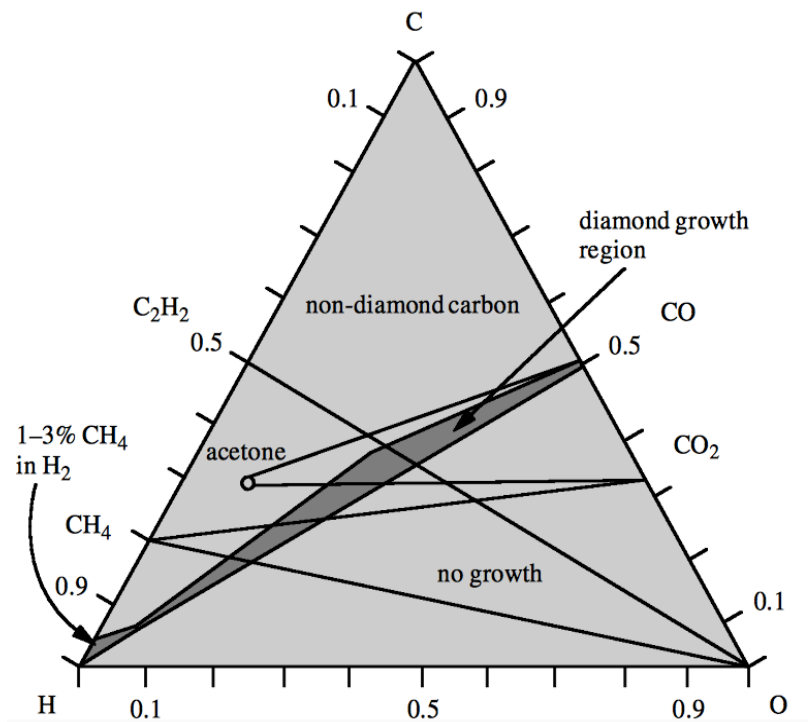
Figure 4. Bachmann triangle composition diagram. Diamond growth detected in specific region above C-O tie-line. Non-diamond species are formed over the specified growth region and no growth is identified below the tie line [19].

Several parameters affect the diamond deposition process by CVD and influence the growth rate and quality of the film including: carbon concentration, substrate temperature and total gas pressure. A substrate temperature increase from 700 to 900 °C results in an exponential rise in the growth rate of diamond from 1 to 5 μm h^{-1} [20]. The crystals are morphologically enhanced and on average have a larger grain size. A higher carbon concentration e.g. methane gas concentration and total gas pressure in the vessel also increase the rate of growth [21]. Additionally, removal of carbon atoms in diamond and graphite by hydrogen atoms is termed etching. Graphitic sp^2 carbon species are etched away at a significantly higher rate than diamond, ultimately, removing graphite, thus permitting further growth of diamond and increasing the purity of the resulting polycrystalline diamond films.

1.3 Crystallography of Diamond and GaN Structures

The deposition and growth of CVD diamond polycrystalline film onto a substrate made from a different material such as GaN is called heteroepitaxial growth. The result of heteroepitaxy of diamond-on-GaN is affected by the compatibility of the two materials [22]. More specifically, the crystallographic features of GaN and diamond such as the lattice constants, crystal structure, atom orientation and diamond growth planes influence the growth of diamond on a substrate other than diamond.

The GaN substrate adopts the Wurtzite crystal structure. In the hexagonal close packed structure (HCP) GaN, every atom is in contact with six other atoms. This is the basal plane for the GaN crystal structure (Figure 5) [23].

Polycrystalline FCC diamond displays 3 distinct crystallographic planes described by 3 integer indices, (100), (110) and (111), where the (111) plane is most suitable for growth on GaN (Figure 5) [24]. Ideally, the diamond layer deposited on GaN should exhibit "a three-fold of six-fold rotational symmetry" [25].

Diamond in the (111) orientation displays a hexagonal atom arrangement and can achieve growth on hexagonal GaN due to the close match in crystal structure and atom orientation [26]. The hexagonal atom arrangement of both materials structurally favours the CVD diamond deposition on the GaN surface and results in two layers that have better adhesion.
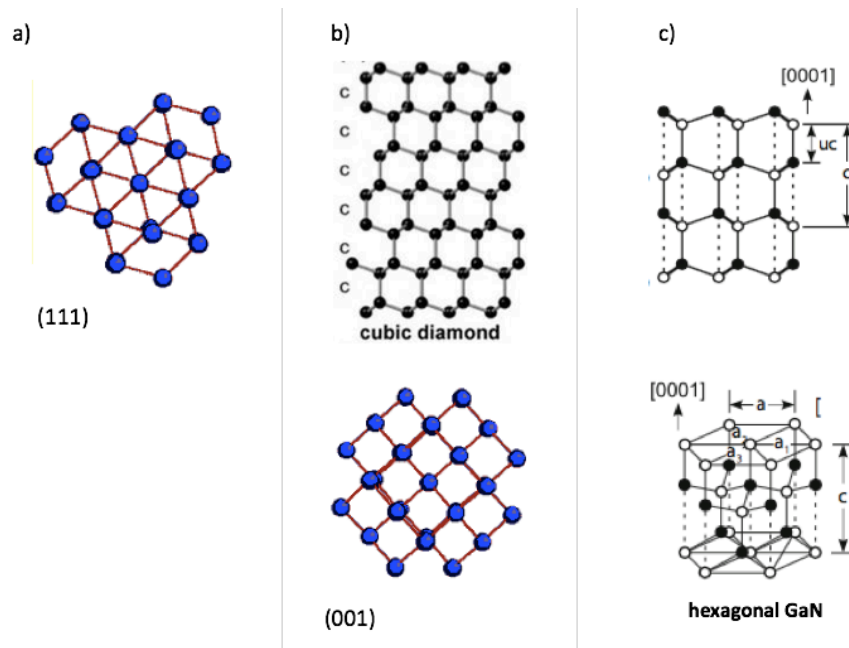

Figure 5. a) Cubic diamond hexagonal atom arrangement in (111) plane
b) Cubic diamond structure and atom arrangement in (001) plane c) Wurtzite hexagonal close packed GaN structure [27] [28].

The heteroepitaxy of the diamond film is also influenced by the lattice constants of the GaN substrate and diamond layer. The difference between the constants is termed the lattice mismatch, where a large magnitude in lattice mismatch results in strain and defects in the heterostructure formed and potential delamination. Additionally, the CVD diamond-on-GaN structure may suffer from diminished thermal properties and structural changes from the high strain [22].

The strain resulting from the high diamond-on-GaN lattice mismatch (89%) can be decreased by the use of a barrier layer *e.g.* SiC between diamond and GaN. This interlayer should ideally have a low lattice mismatch with both the GaN and diamond layer. For instance, SiC lattice mismatch with GaN is 18.9% [9]. A further issue with growing diamond onto a non-diamond substrate is that in order to encourage the diamond to nucleate, seed crystals of nanodiamond need to be deposited onto the surface. These seed crystals are usually composed of detonation nanodiamond of size <10nm, and can be deposited onto the surface in a variety of ways (see section 1.7). Ideally, seeding the surface in these ways should result in a monolayer of close-packed nanodiamond crystals lying on the surface. Diamond CVD then deposits diamond onto these seeds, enlarging them and eventually fusing them together into a continuous layer of diamond on the surface. However, often the seed layer is not as close packed as desired, leaving exposed gaps or windows which expose the substrate to the reactive species present in the CVD gases.

1.4 GaN Electronic Devices

Gallium nitride (GaN) is a semiconducting material that has been steadily receiving more attention in the power electronics industry due to its remarkable material properties, such as high saturation velocity and high breakdown voltage [29]. This superior semiconductor has a large, direct band gap (3.4 eV) permitting its incorporation in high-power and high-frequency devices. GaN-based devices lower resistance giving low conductance losses, and can work at high voltage and outperform traditional Si based devices in speed and power handling. GaN technology is currently found in high power lasers and blue/green LEDs used in traffic lights. Prospective applications involve GaN High-Electron-Mobility Transistors (HEMT) for base stations in 5G next generation wireless mobile devices, satellites and spintronics [1] [30]. Top companies already selling GaN-based devices in an ever-expanding market include Avago Technologies, GaN systems and Qorvo [31].

However, an important issue affecting the reliability for these devices is heat build-up leading to overheating and ultimately to device failure. Localised heat rise in certain areas of the GaN

wafer creates hotspots. This issue reduces a device's life span dramatically and limits these high-power devices to usage at 50% maximum capacity.

Combining a diamond film with the GaN device is a promising method, which aims to reduce the localised heat build up to manageable levels by utilising diamond. Diamond's high thermal conductivity draws heat away from the GaN and spreads it over the entire diamond layer [32].

1.5 Thermal management of GaN-based devices

Although GaN-based electronic devices demonstrate the potential to revolutionize the high-power electronics industry, a tailored solution to the heat build-up issue is required. Integration of diamond polycrystalline films on GaN devices can contribute to heat management and extraction, without altering the chemical composition of the GaN device, as diamond is chemically inert. Diamond is a material with exceptional thermal properties, such as high thermal conductivity k (20 W cm^{-1} K^{-1}) and high thermal stability, withstanding temperatures above 3000 K. An overall significantly low thermal resistance in the GaN-based device can be accomplished by forming a GaN/diamond interface. A CVD diamond layer acts as a heat spreader, where localised heat is conducted from hotspots to the outer sides of the GaN layer (Figure 6). Ultimately, heat is conducted away to a heat sink and can exit the GaN device through a range of methods. Notable methods include the use of a cooling fan, micro-channels containing a cooling fluid or an air-cooled heat sink.
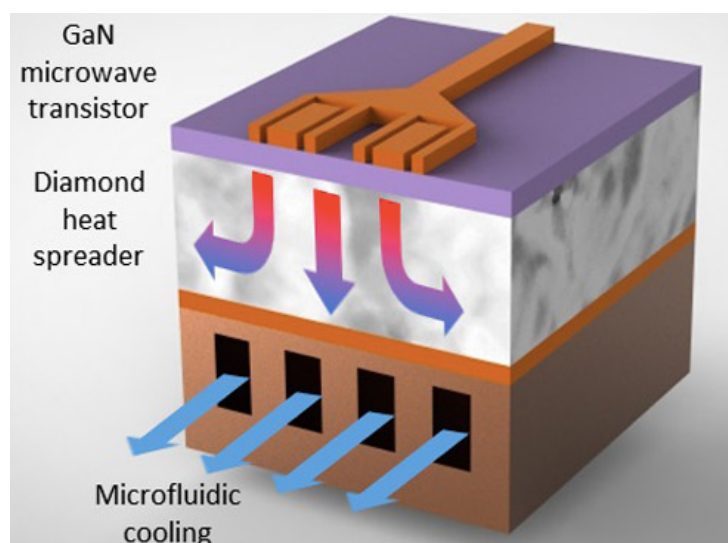

Figure 6. GaN transistor bonded to heat spreading diamond film [33].

Compared to GaN devices using a SiC layer, synthetic diamond films reduce the peak channel temperature by 40% [34]. However, bonding the GaN and diamond layer gives rise to several complications. High temperatures of around 1200 K are required during the CVD process that deposits a diamond film over the GaN surface. Although diamond has a low thermal expansion coefficient 1.1×10^{-6} K^{-1} and therefore slightly contracts with temperature changes, GaN has a relatively larger thermal expansion coefficient of 5.5×10^{-6} K^{-1} and thus contracts significantly upon cooling after diamond CVD. The thermal expansion coefficient mismatch of 81.8% between the two materials contributes to the adhesion and delamination issues detected.

Consequently, the GaN layer is smaller compared to the bonded diamond layer resulting in a bent/bowed wafer and/or a diamond layer that is susceptible to detachment or cracks [35].

In addition to that, any GaN that is exposed (*e.g.* by gaps in the seeding layer) to atomic H from the process gas reacts during the CVD deposition forming gallium droplets and N$_2$ gas. Thus, these reactions with atomic H etch the GaN surface, creating holes and reducing its quality and uniformity, which decreases the ability to grow a smooth diamond layer above [34] [36]. Another issue identified regarding the growth of CVD polycrystalline diamond films is the low thermal conductivity at the base layer, known as the nucleation layer, in contrast to the layers above. This is a direct result of the need to use diamond seeds on a non-diamond substrate. The initial layer of diamond deposited is of poorer quality, as it grows onto the nanodiamond seeds. Thus, the first 10-50 nm or so of the diamond film is composed of small grains with large numbers of grain boundaries which increase phonon scattering and reduce the thermal conductivity of the diamond film.

As the growth of the diamond film progresses, columns of diamond grow up from the base layer. These columns compete against each other for growth space, leading to non-uniform growth cross-section. The net effect is that the grain size increases and thus the quality of the film increases the thicker the film is grown (Figure 7). Although the diamond film as a whole has high thermal conductivity, the poor quality nucleation layer has low conductivity, and even though it is relatively thin, it still acts as a thermal barrier between the main diamond film and the GaN.
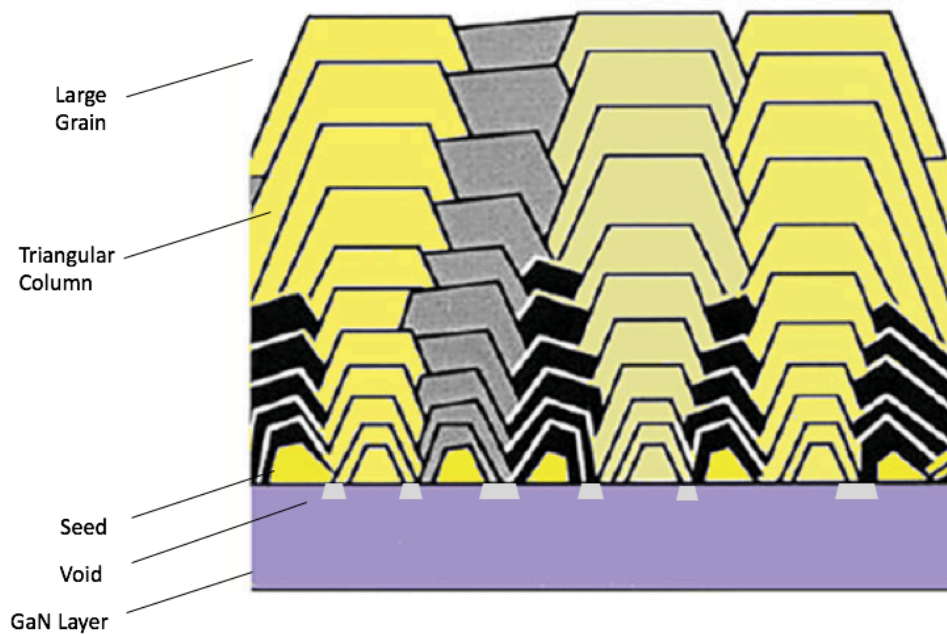
Figure 7. Cross section through the CVD GaN layer noting the voids created by etching, the column growth of diamond and increasing diamond grain size away from nucleation layer [37].

1.6 Barrier Layer at GaN/Diamond Interface

The incorporation of an additional layer between the diamond and GaN has been proposed as a means of improving the GaN/diamond interface. The thin layer of Al, Ti or SiC must be chemically compatible and bond to the two other surfaces, enhancing the close packing of the different layers in the wafer (Figure 8).
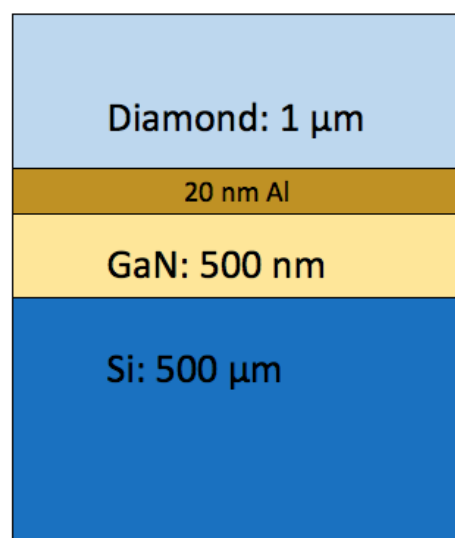
Figure 8. CVD diamond-on-GaN structure bonded by an Al interfacial layer noting the relative thickness of every layer, figure not to scale [32].

Furthermore, better adhesion between the GaN, interlayer and diamond layer can be promoted by the incorporation of an interlayer with relatively similar crystallographic features. SiC is commonly used as an interlayer adopting a hexagonal structure comparable to that of hexagonal close-packed GaN and (111) diamond. SiC has a low lattice mismatch with both the GaN and diamond layer, where SiC lattice mismatch with GaN (18.9%).

Additionally, the interlayer's thermal expansion coefficient should be intermediate to those of diamond and GaN in order to relieve some of the strain induced by cooling. For instance, the interlayer AlN has a thermal expansion coefficient of $4.2 \times 10^{-6} \, K^{-1}$, which is comparable to the values for diamond and GaN, $1.0 \times 10^{-6} \, K^{-1}$ and $5.6 \times 10^{-6} \, K^{-1}$, respectively [9].

Also, a smooth interfacial layer deposited before the growth of diamond by CVD acts as a platform and increases the uniformity of the initial diamond layer deposited.

This layer also serves as a protective layer for the GaN surface as it physically prevents etching from hydrogen atoms. The barrier layer also 'glues' the GaN to the diamond surface, reducing the possibility of detachment.

However, this extra layer has much worse thermal conductivity than diamond, and so reduces thermal conduction to the diamond film. Ideally, the addition of this barrier layer should not greatly increase the thermal boundary resistance (TBR_{eff}) and not reduce thermal conductivity k at the interlayer [32]. To achieve this the thickness of the barrier layer should be minimized. However, the layer should still permit the diamond seeding and nucleation at its surface [38]. Ultimately, these factors contribute directly and indirectly to TBR_{eff} reduction. Recent attempts have been made to remove the interlayer by etching during the growth of diamond film. This approach enhances the bonding at the GaN diamond interface, while eliminating the increase in thermal resistance by the barrier layer. Although this technique is promising, the barrier layer should be etched at a slower rate compared to the rate of diamond deposition to ensure that a compact layer of large grain size diamond crystals deposited can protect the GaN layer from etching [39].

1.7 Surface Pre-Treatment

CVD diamond growth originates at the surface of the GaN layer and thus the features of this surface greatly influence the deposition of the diamond layer. The smoothness, uniformity and packing of the diamond layer can be enhanced by modifying the GaN surface prior to CVD deposition. These modifications potentially change the GaN stress and energy at the surface. Lowering the surface energy difference between diamond and GaN could result in a rise in nucleation [40]. In addition, some modifications aim to increase adhesion between the

distinct diamond and GaN layers and prevent delamination. Pre-treatment of the GaN layer includes physical modification of the surface by methods such as seeding, manual/ultrasonic abrasion and surface patterning.

1.7.1 Seeding

One of the core issues regarding the use of a diamond film as a heat spreader is the low thermal conductivity of diamond at the base layer, where growth originates (see section 1.5). The interface between the diamond and the GaN layers determines the heat conduction between the two. As mentioned previously, the growth of diamond on substrates other than diamond *e.g.* GaN requires seeding. Seeding ultimately improves the grain size and morphology of the first crystals grown, creating a smooth uniform continuous diamond film at the base layer. Seeding methods utilise diamond seeds ranging from nano- to micro-crystalline in size and may be deposited by different methods *e.g.* electrospray or electrostatic self-assembly [41]. One recent method employs a two-step approach, which utilizes a mixture of micro-diamond (~5 μm across) for the first seeding layer, and nanodiamond (~3-5 nm) to fill any voids. This allows for high thermal contact with the microdiamond and enhances the rapid growth of larger crystals in close proximity to the base layer, limiting the formation of voids between the smaller diamonds at the base [42]. Grain boundaries and gaps in the first layers of diamond grown lower the conductivity.

A compact layer of large diamond crystals is highly favourable as less voids form, limiting the surface area of exposed GaN which is otherwise susceptible to etching. Also, the thermal conductivity at the GaN/diamond interface increases as smooth uniform layers of large grain size that have less defects and gaps conduct heat more efficiently.

The zeta (ζ) potential seeding technique focuses on increasing the coverage and density of diamond seeds situated on the GaN layer. This technique exploits the electric potential between the GaN layer and nanodiamond particles at the interface. It is important to note that the GaN crystal structure has two separate faces which either consist of Ga or N atoms and thus have an inequivalent charge state. Therefore, depositing nanodiamond seeds of opposite charge to the suitable face of GaN can lead to self-assembly of the nanodiamonds and a high seed density on the GaN surface. Nanodiamonds suspended in a suitable liquid, such as water can be terminated with- OH or -COOH groups and become negatively charged, or with -H to become positively charged.
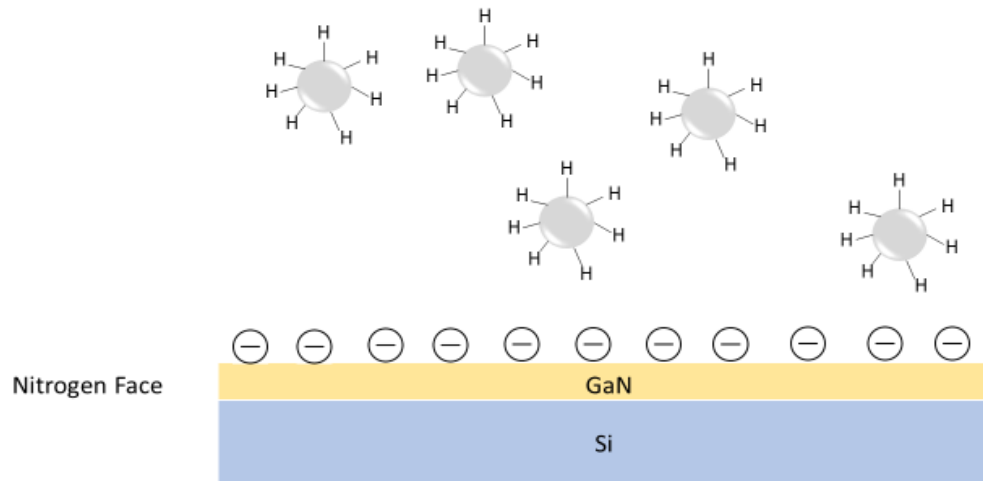
Figure 9. Hydrogen terminated nanodiamonds displaying a positive zeta potential value ζ attracted to the nitrogen face of the GaN layer that has a negative zeta potential value ζ at pH~7 [43].

The overall electrostatic surface potential of the nanodiamond particles in the suspension is termed the surface zeta potential ζ, and the sign and magnitude of ζ indicates the electrical stability between the GaN surface and the charged diamond seeds.
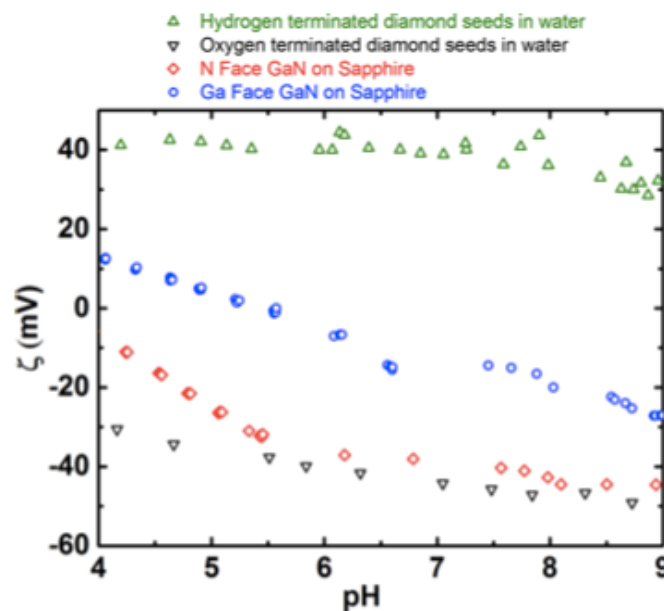
Figure 10. Zeta potential ζ vs pH for diamond seeds terminated with hydrogen and oxygen and for nitrogen and gallium faces of GaN in H_2O [40].

Despite the fact that the ζ fluctuates as pH varies from 4 to 9, the value of ζ for the diamond seeds and GaN faces at pH ~7 is considered the most useful, because (neutral) H_2O is a common solvent for diamond seeding suspensions (Figure 10).

Maximising the zeta potential difference of opposite polarity is ideal in promoting the self-assembly of charged nanodiamonds [40]. At pH ~7, hydrogen-terminated seeds have a positive zeta potential ζ (+40 mV) and 'stick' to both the Ga and N faces that have negative zeta potential ζ values (-10 mV, -35 mV, respectively). The N-face has a negative zeta potential that is higher in magnitude compared to the Ga-face and is ideally seeded with positively charged nanodiamonds *e.g.* H-terminated nanodiamonds. At pH ~7 oxygen-terminated seeds have a negative zeta potential ζ (-40 mV), the Ga-face and N-face also have negative zeta potential ζ values and therefore O-terminated seed self-assembly is disfavoured on both faces. Self-assembly of O-terminated seeds is only favoured in acidic conditions pH ~5 on the Ga-face, as the O-terminated seeds have a negative zeta potential (-30 mV) and the Ga-face has a positive value (+10 mV).

Commonly, the diamond heat-spreading layer is deposited on the N-terminated face, while the GaN HEMT is in contact with the Ga-terminated face.

1.7.2 Manual and Ultrasonic Abrasion

Another technique modifies the surface of the GaN substrate prior to the seeding step, which is in turn followed by the CVD process. This pre-treatment scratches and damages the GaN surface. This may be achieved by manual abrasion with a diamond grit, an extremely harsh method, which causes damage to the GaN layer rendering this method inappropriate for use in creating GaN devices.

Ultrasonic abrasion is a gentler alternative method that enhances nucleation at the surface through a diamond powder suspension [44]. This procedure has been found to increase the nucleation density at the substrate surface to values around 10^{10} cm^{-2} [45], but is still rather too harsh for use with delicate electronic structures.

1.7.3 Surface Patterning

Thermal expansion coefficient mismatch between the diamond and GaN causes stresses and wafer bow, and in the extreme case this can lead to cracking or delamination of the diamond layer. Prevention of delamination is critical for the diamond heat spreader to function. The issue is that GaN and diamond are not chemically reactive toward each other, meaning they tend not to stick together strongly. Under CVD conditions, chemical bonds between C and

Ga and C and N will form, but these tend to be weaker than the C-C bonds in the diamond of Ga-N bonds in the GaN. Thus the diamond-GaN interface is always a chemically weak link. This can be improved using interlayer such as AlN or SiC (see section 1.6) which bond strongly to both diamond and GaN, gluing the two together, but at the expense of increased *TBR_eff*.

A more calculated approach to improve the adhesion between the GaN and diamond layer without using a barrier layer is to use surface patterning. This technique etches suitable corrugations on the GaN surface, yielding an interface that physically locks the two materials together giving a greater ability to withstand the residual stresses.

Initially, the GaN surface is coated with a photoresist, and exposed to UV light. The light-sensitive photoresist on the unmasked parts of the surface polymerizes upon exposure to UV light and baking in the unmasked parts of the surface [46]. A solvent *e.g.* acetone, then dissolves any unpolymerised photoresist leaving polymerised photoresist structures on the GaN surface. Subsequently, a plasma etching system using an etching gas *e.g.* Cl_2, SF_6 etches the exposed GaN surface, creating defined corrugations (Figure 11) [47] [48]. Diamond CVD onto this corrugated surface results in a diamond layer which tightly interlocks with the GaN layer at the grooves, therefore minimizing the effects of the large lattice mismatch (89%) and thermal expansion coefficient mismatch (81.8%) between GaN and diamond. The GaN "locks into" the diamond because it shrinks on cooling more than diamond.
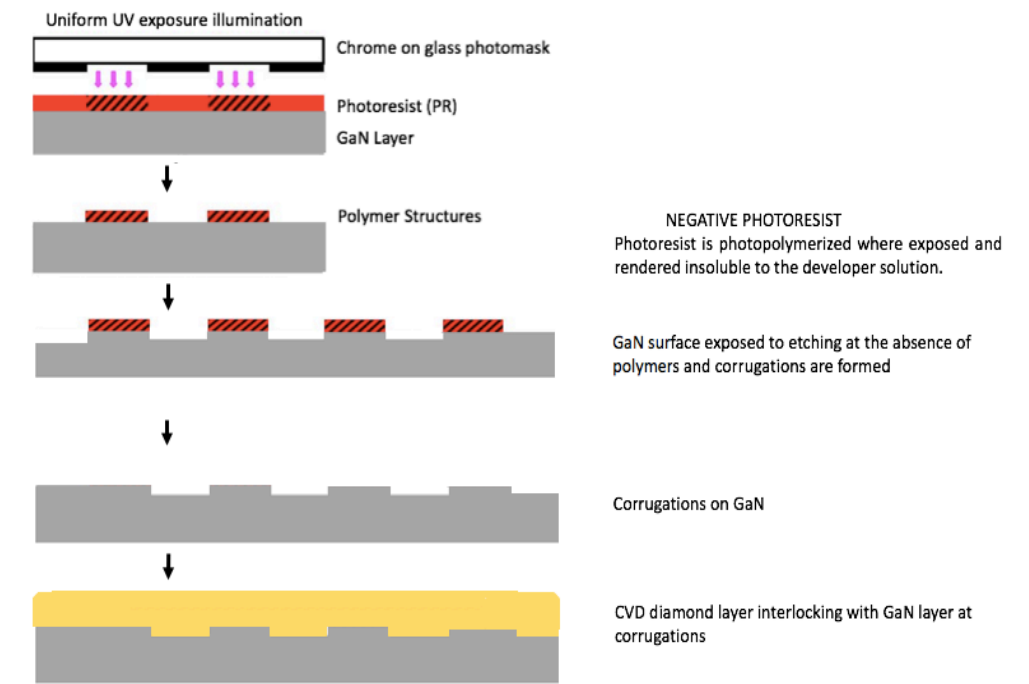
Figure 11. GaN surface patterning through the use of negative photoresist followed by etching and growth of CVD diamond layer, interlocking with the GaN layer at corrugations [49].

1.8 Heat Removal from GaN Devices via Microchannel Heat Sinks

Localised heat in thermal hotspots is conducted rapidly through the diamond heat spreading layer towards the back of the device, and passed to some type of heat sink or radiator. To achieve an overall reduction in the high-power device's operating temperature, the heat sink ultimately absorbs heat and releases it to the surroundings in an efficient manner.

Integrating a fan blowing onto a heat sink is a common air-cooling method employed in GaN high-power devices. The difference in temperature between the heat sink and the surroundings facilitates heat dissipation away from the device [50].

Another method of effective heat dissipation out of the device involves a network of microchannels parallel to one another, where cooling fluid flowing inside the channels absorbs the heat from the heat sinks. The heated fluid ultimately flows through a radiator, cools down and is able to flow back through the channels to absorb more heat.

The heat sinks are carried by a substrate such as, an aluminium cold plate that is added to the GaN device. Alternatively, the microchannel network can be fabricated into the inactive part of the GaN device [51].

1.9 Conclusions

GaN-based high-power electronic devices exhibit promising future prospects in the electronics industry due to outstanding properties such as high breakdown voltage and high saturation velocity. At present these devices are limited by poor heat dissipation and overheating, leading to device malfunction and reduced lifetime. A diamond thin film deposited by CVD onto the GaN layer serves as a heat spreader that rapidly conducts heat from localized hot spots towards a heat sink, where heat can dissipate out of the device.

However, there are a number of problems associated with fabrication of this GaN-diamond layer. Delamination between the GaN/diamond layers is commonly observed due to a large mismatch in lattice constants and thermal expansion coefficients. Adhesion at the GaN/diamond interface can be improved by modification of the GaN surface prior to CVD diamond growth. GaN surface pre-treatment techniques include ultrasonic abrasion, seeding and surface patterning with photoresist. Another proposal aiming to improve the adhesion of GaN and diamond layers and release interfacial strain involves the addition of an extra barrier layer in between the GaN and diamond layers. This literature review will be followed by an experimental exploration of various methods discussed above regarding the growth of high-quality CVD diamond-on-GaN for thermal management.

2. Experimental Methods and Techniques

2.1 Project Aim

The experimental part of this investigation focuses on the incorporation of an interlayer between the GaN and diamond layers in order to improve adhesion at the interface between the layers. The aim is to identify the thickness of interlayer that provides a smooth, uniform continuous layer over GaN and chemically bonds the diamond and GaN surface, thus creating a strong chemical interface that can withstand compressive stress. The interface should ultimately prevent the formation of cracks and delamination of the deposited diamond layer. However, it is important to note that as the interface thickness increases, the thermal conductivity at the interface is compromised as this extra layer has much worse thermal conductivity than diamond, and so reduces thermal conduction to the diamond film.

2.2 Sample Preparation

In this investigation the samples used were cut out in $1cm^2$ pieces using a diamond scribe from a wafer containing high purity gallium nitride of 4.28 μm thickness on a 4-inch silicon layer. The samples prepared for all diamond growth experiments were cut from the same wafer (wafer code GCAMBA2057) in order to reduce discrepancies between the samples and control this variable.

2.2.1   Electrospray Seeding

The GaN-on-Si samples were seeded with a two-step approach which utilizes a mixture of micro-diamond (~5 μm across) for the first seeding layer, and smaller nanodiamond
 (~3-5 nm) to fill any voids. This allows for high thermal contact with the microdiamond and enhances the rapid growth of larger crystals in close proximity to the base layer, while reducing the area of GaN surface exposed to H etching. A micro-diamond suspension was prepared in methanol and then agitated using an ultrasonic probe (30 mins). Sonication stabilizes the solution and separates agglomerates. A nanodiamond suspension was also prepared in methanol and then agitated using an ultrasonic probe (30 mins). The electrospray technique was used to seed the samples. The samples were mounted onto a holder with a rotating disc powered by a motor with ~100 rpm rotational speed (Figure 12). The samples spun at a moderate speed resulting in uniform seeding, while minimizing the possibility of detachment from the rotating disc. A high voltage (35 kV) was applied to the tip of the syringe containing the microdiamond suspension resulting in ionization of the suspension, where the suspension sprays across the chamber, and evaporates, depositing microdiamond

seeds onto the samples [52]. The technique was repeated using the nanodiamond suspension. Every GaN-on-Si sample was seeded with a thin layer of a mixture of microdiamond and nanodiamond prior to CVD diamond growth in the microwave plasma-enhanced CVD reactor.
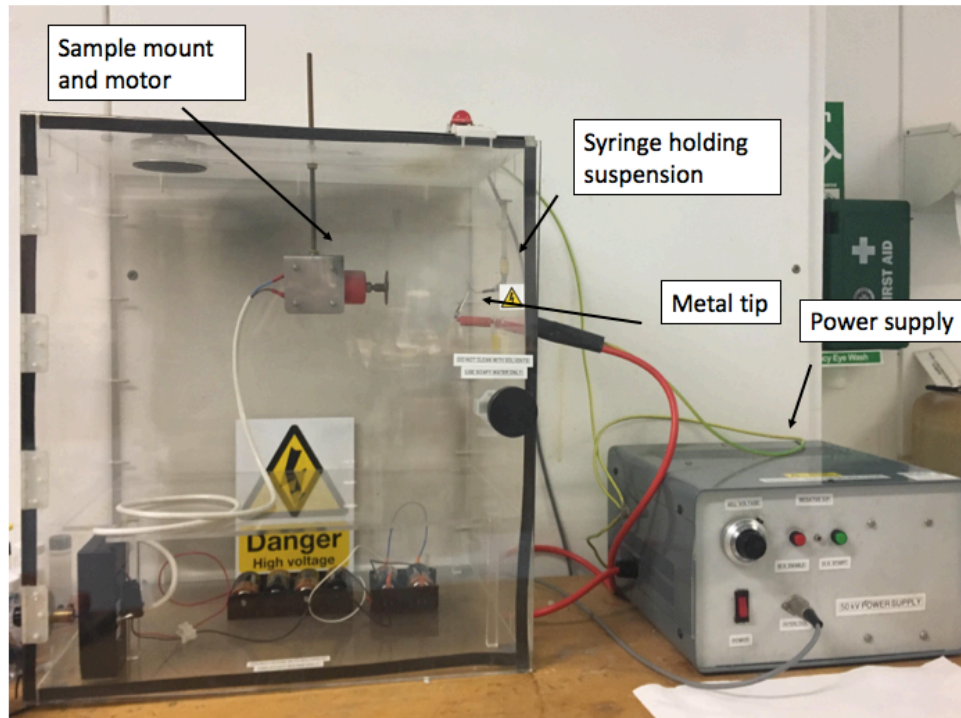
Figure 12. Diagram of the electrospray kit used for the mixed diamond seeding of GaN-on-Si samples [43].

2.2.2 Evaporator Coater

A thin layer of aluminium was deposited on seven GaN-on-Si samples prior to the mixed seeding by electrospray. The evaporator coater consists of a vacuum pump that pumps down the chamber to 6.0×10^{-2} mbar pressure. The resistive double loop tungsten wire was wrapped with an Al wire of thickness 0.71 mm, where Al was deposited onto the samples by flash evaporation. The tungsten wire was heated, causing the evaporation and deposition of Al particles onto the GaN-on-Si samples placed a few cm below the wire (Figure 13). The vacuum established minimizes the presence of background vapours inside the chamber and promotes the direct and rapid condensation of Al particles onto the samples, limiting collisions with background gas particles. The build-up of vapour gas in the chamber increases the pressure and reduces the vacuum quality. The presence of a high vacuum is essential for uniform and regular coating. Collisions with background gases lead to deposition of contaminated materials by chemical mixing, other than pure Al and hinder the rate of deposition. A thickness monitor displayed the thickness of

the Al coating during the deposition, determined from the mass deposited and the density of Al (2.7 g cm⁻³). The thickness and rate of deposition was controlled, where a slow rate of deposition resulted in a smoother layer of Al, which is important as seeding follows the deposition of the Al interlayer. The presence of a smooth Al layer facilitates the formation of a continuous layer of mixed diamond seeds on the Al interlayer by electrospray seeding.
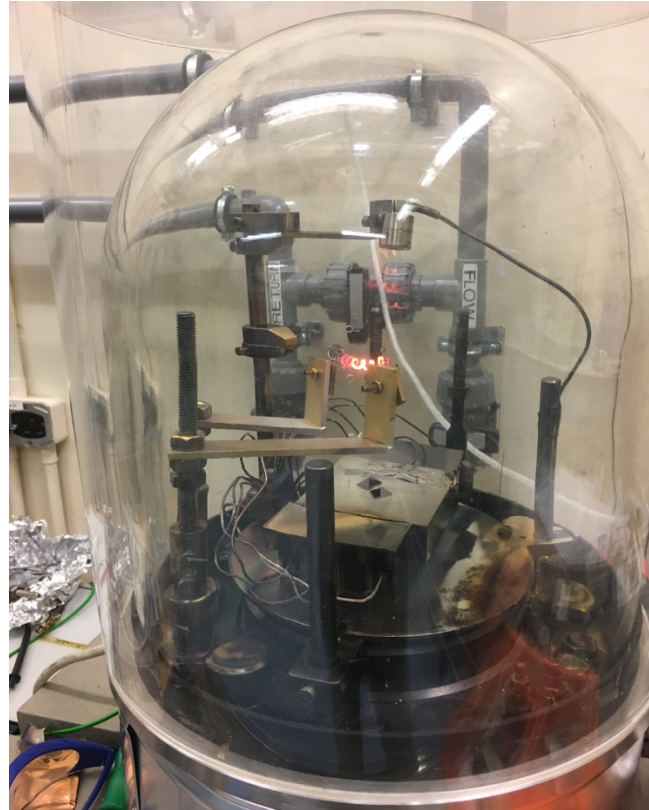
Figure 13. Deposition of Al coating on GaN on Si samples using the evaporator coater [43].

2.3 Microwave Plasma-enhanced CVD Reactor

In this investigation the 1.5 kW ASTeX style Microwave reactor connected to an Al chamber was used for all experiments regarding diamond growth on GaN-on-Si samples (Figure 14). The steel reaction chamber was left under vacuum (0.025 Torr) when not in use to reduce contamination by background gases such as oxygen and moisture [53].

At atmospheric pressure in the chamber the GaN-on-Si sample was placed centrally on a tungsten disk which was itself thermally decoupled from the chamber base with a 50 μm thick molybdenum wire underneath it. After sample loading, atmospheric gases were evacuated from the chamber by pumping down to reach the base pressure. The air blower and water pumps were turned on to ensure that the chamber does not overheat during the growth. Hydrogen gas (flow rate: 300 standard cubic centimetres per minute (sscm)) was introduced

in the chamber, heated and excited by microwaves at low (15 Torr) pressure and striking power was set to 45%. A violet/white plasma ball, appeared above the sample. The white region was caused by carbon containing radicals in the chamber. Methane gas (flow rate: 12.5 sscm) CH_4 4% in H_2 was also introduced ensuring the growth of good-quality diamond at a moderately high growth rate, as increasing carbon concentration results in faster growth rates. The pressure and power were set and maintained at the standard growth conditions selected of 110 Torr and 1100 W, respectively, based on previous trial and error attempts of CVD diamond deposition on GaN and Al. The temperature evolved by the sample was relatively variable between runs under the standard conditions noted in the range of 700-740 °C. The balanced temperature of 700 °C ensured that the diamond grown was of good quality and was not compromised by a slow growth rate, as a higher temperature speeds up the growth rate but results in the deposition of poor quality diamond. This fluctuation of $\pm$ 40 °C can be rationalised as the temperature probe does not measure temperature directly. The pyrometer measures the IR light emitted from the sample, which can be affected by numerous other factors and therefore the temperature readings fluctuate.

All growth runs had duration of 6 h under the specific standard conditions summarised below:

Table 2. Standard conditions used for CVD diamond growth with microwave plasma-enhanced CVD reactor.

Conditions/Units	Value
Pressure/Torr	110 $\pm$ 0.3
Base Pressure/Torr	0.29 $\pm$ 0.3
Power	1100 W
Temperature of Sample/ °C	700 $\pm$40 °C
Emissivity (EMS)	0.15
Flow rate H_2/sscm	300
Flow Rate CH_4/sscm	12.5

Control samples of diamond were grown under the same standard conditions on GaN on Si unseeded wafers. Control samples were also grown on Si wafers under standard conditions with modifications on EMS and the temperature of sample evolved, where Emissivity = 0.13 and Temperature 640 °C.
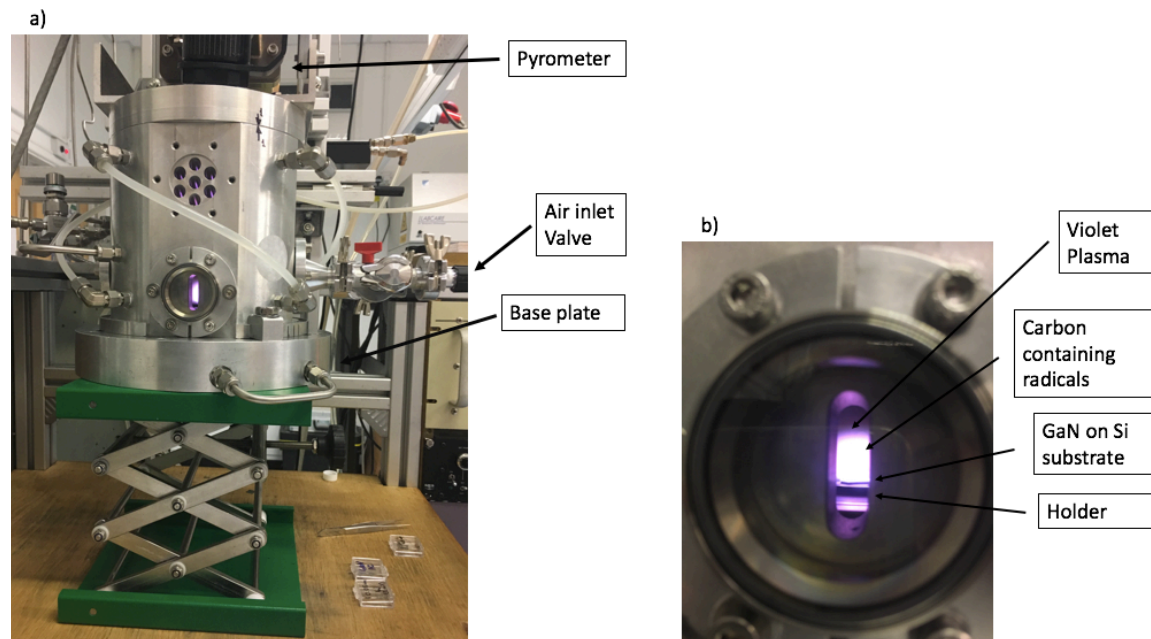
Figure 14. a) Diagram of Al reactor chamber, b) Plasma 4% CH_4 in H_2 during diamond CVD growth run [43].

2.4 Sample Characterization and Analytical Techniques

2.4.1 Scanning Electron Microscopy

The topography of the diamond-on-GaN samples was captured in images produced by Scanning Electron Microscopy (SEM) at the University of Bristol Chemical Imaging Facility. The samples were placed on the sample holder at a 75° angle to enable the viewing of the diamond surface texture and composition from a slanted perspective. The chamber was pumped down to vacuum and a 15 kV focused electron beam hit the surface of the sample. The electrons that hit the sample surface bounce back producing a signal that is received by detectors and in combination with the position of the focused electron beam produce an image of the sample surface.

The JEOL JSM-IT300 produced images in the range of 500 to 2000 × magnification for the five samples. The SEM images provided insight on the size and morphology of diamond crystals, the uniformity of the diamond layer deposited, the delamination of the diamond layer and the impact of CVD diamond growth on the GaN surface.

2.4.2 Raman Spectroscopy

Raman Spectroscopy was used to qualitatively characterize the samples following CVD growth in order to identify the allotropes of carbon formed. The observation of a narrow peak at 1332 cm^{-1} indicates the presence of sp^3 hybridized diamond. Other peaks at 1582 and 1350 cm^{-1} exist due to sp^2 C-C bond vibration in carbon structures grown by CVD that are graphite-like and disordered sp^2, respectively. The peak heights of the various Raman lines identified can be compared in order to determine the relative ratio of diamond sp^3 C to graphitic sp^2 carbon species present on the GaN sample. The Full Width at Half Maximum (FWHM) was determined for the diamond peaks, which is a rough indicator of the strain in the samples in this study. This investigation used the Renishaw 2000 spectrometer with a laser at 514 nm wavelength causing excitation at 10% laser power.

2.4.3 X-ray Tomography

X-ray Tomography XRT is a cutting-edge, non-destructive, analytical technique that computationally combines a number of 2D projections of a sample to produce a 3D model and visualize the internal structure of the sample. An X-ray point source fires X-rays at the sample and a detector measures the decrease in the X-ray intensity as it interacts with matter, called attenuation [61]. The sample stage holding the sample is mobile and is rotated by 1 degree approximately 360 times to capture a series of 2D images. A high aspect ratio is more suitable for modelling of planar samples, where more X-ray imaging is performed on the long axis of the sample.

Diamond samples were characterized using 3 Watts Power, 40 kV Voltage and an exposure time of 4 secs.

The Xradia Versa 3D X-ray Microscope (XRM) was used for all samples analysed by XRT in this investigation (Figure 15).
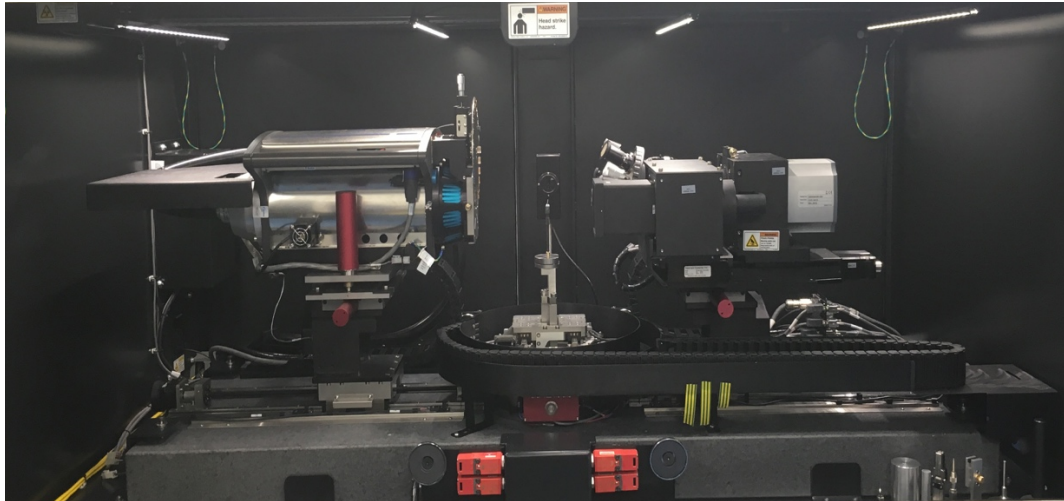
Figure 15. The Xradia Versa 3D X-ray Microscope (XRM) [43].

3. Results and Discussion

CVD diamond was grown on GaN-on-Si samples under the standard conditions noted in Table 2 in order to limit the effect of other variables on the outcome of the diamond growth runs performed. Fluctuations in conditions such as gas flow rates, temperature, power and pressure may increase or decrease the quality of the diamond layer deposited and the adhesion to the GaN or interface surface. Any inconsistency in reactor conditions would deem it impossible to identify the effect of the variable factor explored in this study. The variable factor was the thickness of the interfacial layer between the GaN and the deposited diamond layer. Diamond was deposited on two duplicate GaN on Si samples, where each sample was coated with an Al interfacial layer of varying thickness. The thicknesses of the Al interlayer used were 1.5, 5.5, 20.0, 40.3 nm. Diamond was deposited on a GaN on Si sample with no interlayer and was used as a control sample.

The following table provides an overview of all the growth runs in this investigation, focusing on delamination and cracks observed on the samples (Table 3).

Table 3. Overview of samples in CVD diamond growth runs.

Sample Name	Substrate	Interlayer Material	Interlayer thickness/ nm	Observations
Si control	Seeded Si wafer	-	-	No delamination
GaN control	GaN on Si wafer	-	-	Delamination on the edge and crack
GaNAl_1.5.1	Seeded GaN on Si wafer	Al	1.5	Smooth diamond film deposited
GaNAl_1.5.2	Seeded GaN on Si wafer	Al	1.5	Delamination on the edge and crack along the side
GaNAl_5.5.1	Seeded GaN on Si wafer	Al	5.5	Smooth diamond film deposited
GaNAl_5.5.2	Seeded GaN on Si wafer	Al	5.5	Severe delamination and cracks along middle of sample
GaNAl_20.0.1	Seeded GaN on Si wafer	Al	20.0	Smooth diamond film deposited
GaNAl_20.0.2	Seeded GaN on Si wafer	Al	20.0	Smooth diamond film deposited
GaNAl_40.3.1	Seeded GaN on Si wafer	Al	40.3	Smooth diamond film deposited

3.1 CVD Diamond Growth on GaN without an interlayer

The fist part of the experimental part of this investigation involved the growth of diamond directly on a GaN-on-Si sample that does not contain an interlayer. This control sample was used as a baseline to compare the outcome of growth runs that involve samples with an interlayer. By visible inspection the growth run resulted in the deposition of a diamond layer as predicted. The formation of a weak interface between GaN and diamond is predicted as gallium carbide and/or nitrogen carbide are not formed, which contributes to weak chemical bonding holding the two layers together. Gallium and nitrogen that form the GaN wafer do not participate in chemical bonding with the diamond as that would result in the formation of metal gallium droplets and nitrogen gas, leading to the destruction of the GaN wafer.

3.1.1 CVD Diamond Growth on GaN without an Al interlayer

3.1.1.1 SEM Imaging Characterization

The control samples were imaged by SEM at a 75 ° angle at 250 ×, 1500 × and 2000 × magnification and provided an insight on the extent of diamond coverage of the GaN surface, diamond growth and grain size. Delamination and cracks formed on the diamond film were inspected as well as the changes in the GaN surface post-growth.

SED 10.0kV WD28.9mm Std.-P.C.36.0 HighVac. x1,500 10um
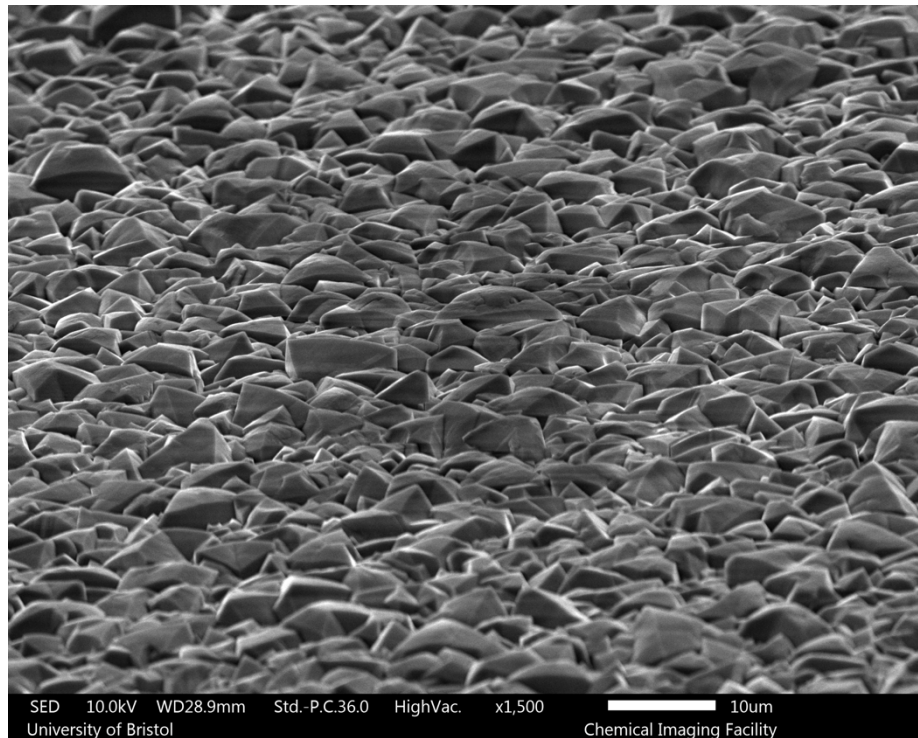University of Bristol Chemical Imaging Facility

Figure 16. SEM Image at 75° angle and 1500 × magnification of diamond surface on GaN control sample without an interlayer.

The 6-hour CVD growth run resulted in the formation of a continuous diamond film that had high coverage of the GaN sample surface. No voids or gaps were visible in the diamond layer, which can be attributed to the mixed microdiamond and nanodiamond seeding method used in the sample preparation. As seen in Figure 16 microdiamonds are greater in size than nanodiamonds and facilitate the growth of diamond grains of larger size at the base layer that have a high thermal contact with GaN and increase thermal conductivity k.

The nanodiamonds cover the gaps between the microdiamonds ensuring the formation of a continuous diamond layer. Charging can be observed in the contrast of the sample images attributed to the accumulation of charge in the sample after electrons hit the diamond surface. Diamond is an insulating material that does not allow a great number of electrons to escape the surface after irradiation. To reduce charging a conductive gold tape can be attached to the sample holder prior to SEM imaging.
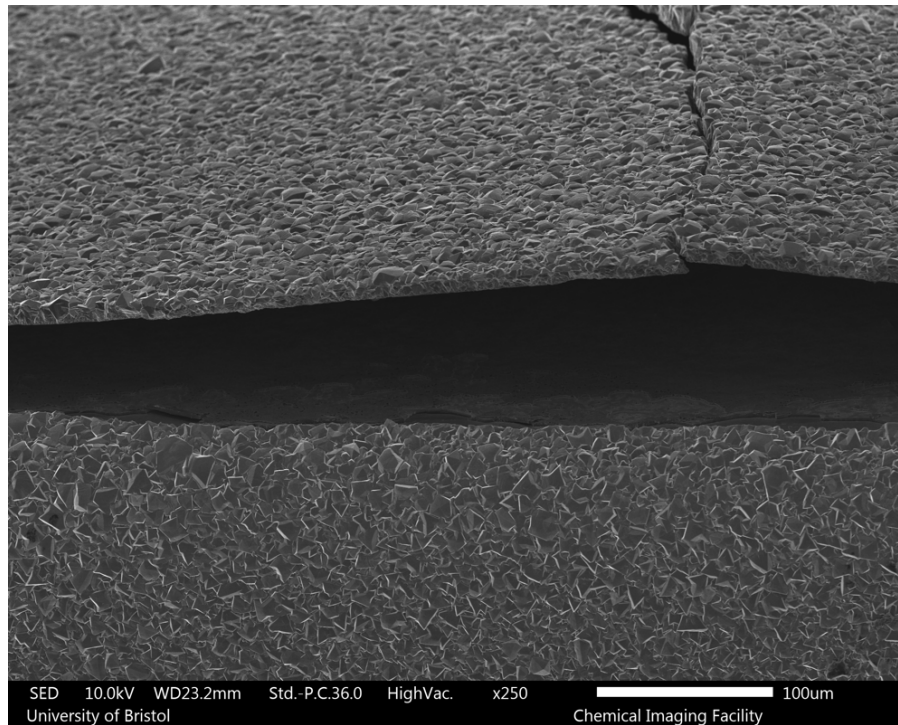
Figure 17. SEM Image at 75° angle and 250 × magnification of delaminated diamond layer on the edge of GaN control sample without an interlayer. Diamond was deposited on the surface and side of the sample.

SEM imaging at a low 250 × magnification displayed the delamination of the diamond film from the GaN surface, as expected in Figure 17. Diamond has a low thermal expansion coefficient 1.1×10^{-6} K^{-1} and therefore slightly contracts with temperature changes. GaN has a relatively larger thermal expansion coefficient of 5.5×10^{-6} K^{-1} and thus contracts ~5.5 times more than diamond upon cooling after the diamond CVD run. Figure 18 suggests that in this growth run delamination occurred during cooling of the sample due to compressive stress and not during the CVD run as there is an absence of large fully formed diamond grains on the delaminated edge of the diamond layer. Delamination during the growth would permit the growth of diamond grains on the delaminated diamond edge of the film. It is hypothesized that without an interlayer diamond grows as a separate, independent film on top of the GaN without chemically bonding to each other. Therefore, the maximum compressive stress was induced at the interface during cooling and not during the growth.

Figure 16 also enables imaging of the GaN surface post-growth, where directly beneath the delaminated diamond film, the GaN surface has been exposed to etching by H atoms. Etching results in the formation of gallium droplets and N_2 gas, negatively impacting the quality and uniformity of the GaN layer.
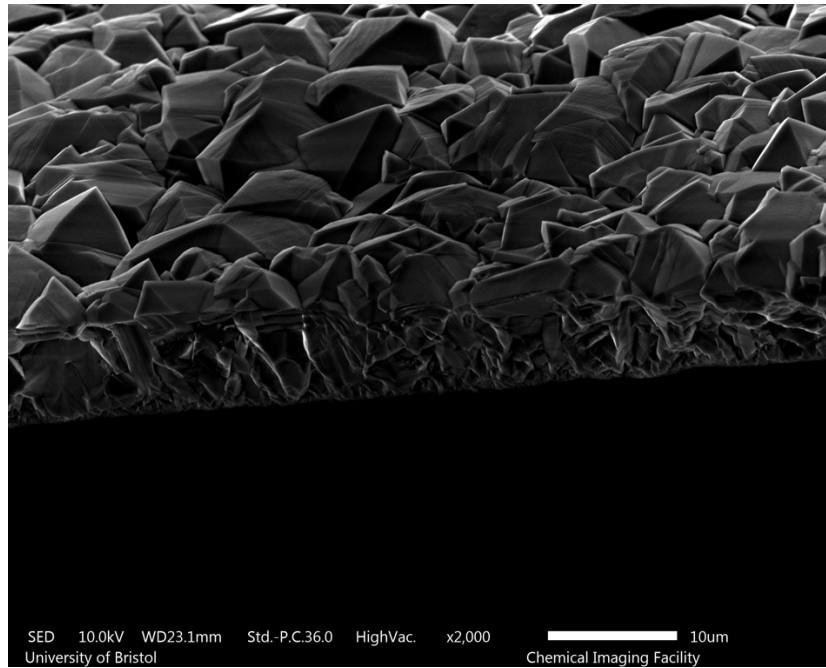
Figure 18. SEM Image at 75° angle and 2000 × magnification of delaminated diamond film on GaN control sample without an interlayer.

The average thickness of the diamond layer based on SEM imaging considering the 75° angle of the GaN control sample was estimated ∼ 6.8 μm by taking measurements at different parts of the layer in Figure 18.

3.1.1.2 XRT Imaging Characterization

The GaN control sample was characterized by X-ray tomography producing images of different cross-sections of the sample and a 3-D model. These were utilized to investigate the quality of adhesion between the GaN and diamond layers, delamination, voids in the constituent layers and post-growth effects on the surfaces of the layers.
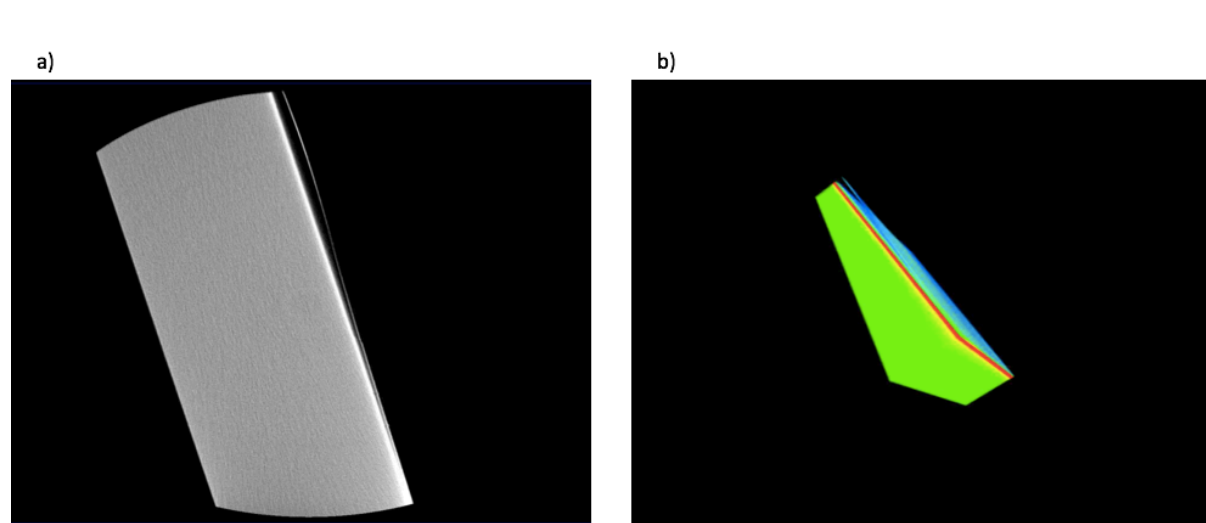

Figure 19. a) XRT image of side-view of GaN control sample b) XRT 3-D model of GaN control sample showing a green Si layer, a red GaN layer and a light blue diamond layer.

Figure 19 a) displays a very thin diamond layer that has delaminated coloured white on a thick 4-inch Si wafer coloured grey. The CVD diamond growth did not significantly impact the GaN layer coloured white negatively, which is uniform, continuous and bonded to the Si wafer. No gaps were identified in the GaN layer, which suggests that the GaN layer was not greatly exposed to H etching during the CVD diamond growth. The small extent of H etching and the high quality of the GaN layer confirms the hypothesis made, based on the SEM image in Figure 18, that the delamination occurred during cooling and not during the growth run. Figure 19 b) is a 3D-model of the GaN control sample displaying the side of the sample formed by a green Si layer, a red GaN layer and a light blue diamond layer. The Si, GaN and diamond layer are closely-packed at the non-delaminated part of the sample. The diamond film shown in blue has clearly delaminated on one side of the GaN control sample as initially hypothesized and explained in detail in section 3.1, as there a large thermal expansion coefficient mismatch between GaN and diamond and weak chemical bonding between the layers.

3.1.1.3 Raman Spectroscopy

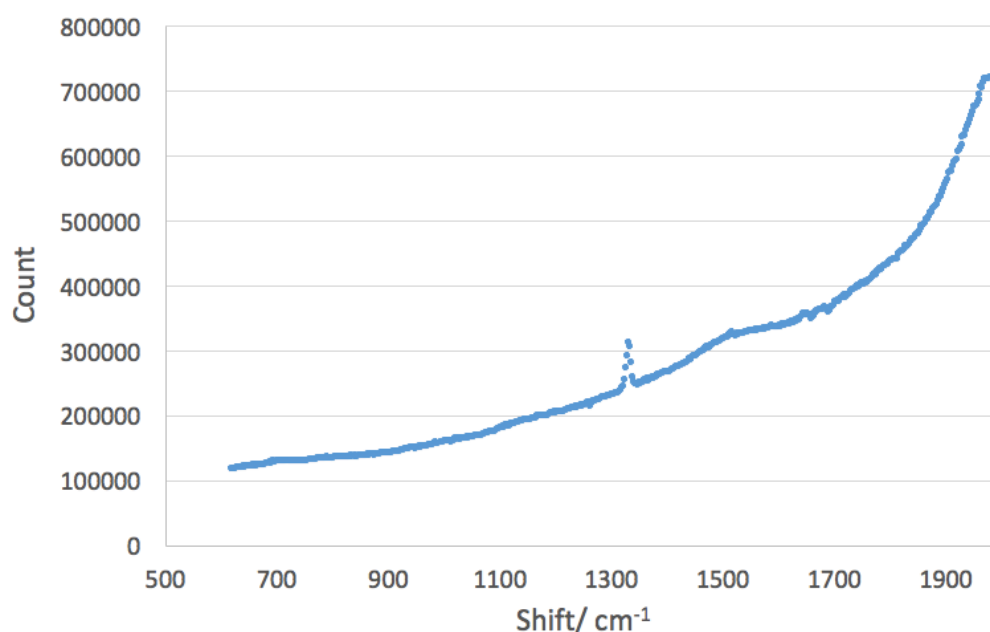Figure 20. Raman spectrum of the GaN control sample without an interlayer after CVD diamond growth run obtained using a laser at 514 nm wavelength.

An intense sharp peak at 1332 cm^{-1} in the Raman spectrum (Figure 20) due to the sp^3 C-C bond vibration indicated the deposition of diamond after the 6-hour growth. As expected, a smaller, less intense broad peak is present at 1580 cm^{-1}, which is characteristic of the

graphitic sp^2 C-C bond. The Full Width at Half Maximum (FWHM) was also determined using a 100% Gaussian fit on the 1332 cm^{-1} diamond peak in Figure 20. The FWHM value provided insight regarding the strain on the sample after the CVD diamond deposition. However, the correlation between FWHM and strain is not strong and should be regarded as a rough indicator of strain in the sample. The FWHM for the GaN control sample was 9.37 cm^{-1} and was the highest FWHM value determined after obtaining a FWHM value for all samples in this study. The highest strain was expected in the GaN control sample as the absence of an interlayer increases the interfacial stress between the diamond and GaN layers, as there is large thermal expansion coefficient and crystallographic mismatch between the diamond and GaN [54] [55].

3.2 CVD Diamond Growth on GaN with an Aluminium interlayer

Delamination issues were predicted to be reduced with the incorporation of the barrier layer at the diamond and GaN interface. The barrier layer alleviates interfacial stress and strengthens the chemical bonding between the GaN and diamond surfaces. The aluminium layer induces the formation of aluminium carbide that increases the close-packing of the constituent layers and lowers the possibility of delamination and formation of cracks. It should be noted that aluminium has a thermal expansion coefficient of 24.4×10^{-6} K^{-1}, which is much greater than the thermal expansion coefficients of diamond and GaN, 1×10^{-6} K^{-1} and 5.6×10^{-6} K^{-1} respectively [56]. Compressive stress present at the interface during cooling after the CVD growth isn't alleviated by the aluminium interlayer and is actually increased by incorporating the interlayer. The formation of species such as aluminium carbide between the GaN and diamond layer reduce the interfacial compressive stress by reducing the thermal expansion coefficient mismatch between GaN and diamond. The thermal expansion coefficient of aluminium carbide cannot be found in literature and is estimated to be comparable to the value for silicon cabide around 2.8×10^{-6} K^{-1}, lying in-between the values for GaN and diamond [57]. Aluminium interlayers of varying thickness were explored.

3.2.1 CVD Diamond Growth on GaN with 1.5 nm Al interlayer

The two samples coated with a 1.5 nm Al layer displayed a varying outcome regarding the adhesion of the GaN and diamond layers. The extra Al layer has much worse thermal conductivity than diamond, and so reduces thermal conduction to the diamond film. Ideally, the addition of this barrier layer should not greatly increase TBR_{eff} and not greatly reduce thermal conductivity k at the interlayer. To achieve this the thickness of the barrier layer

should be minimized and therefore the samples coated with the thin 1.5 nm interlayer were used first for CVD growth in the experimental part of this investigation.

The delamination on the edge of sample GaNAl_1.5.1 was visible after inspection by the naked eye. This was expected as a 1.5 nm has very low thickness and does not coat the GaN with a smooth, continuous atomic layer of Al. Therefore, the diamond growth was initiated on a non-uniform layer of Al contributing to the poor adhesion between the interlayer and the diamond film and the decreased uniformity of the diamond layer deposited. The 1.5 nm interlayer was potentially too thin to chemically bond the diamond and GaN surface by forming aluminium carbide, which enhances the close packing of the layers at the interface and relieves compressive stress upon cooling. Therefore, similar to the GaN control sample without an interlayer, the diamond grew as a separate, independent film on top of the GaN without chemically bonding to the GaN layer. The compressive stress induced at the interface during cooling, and not during the growth, caused the crack and delamination at the side of the sample in Figure 21.
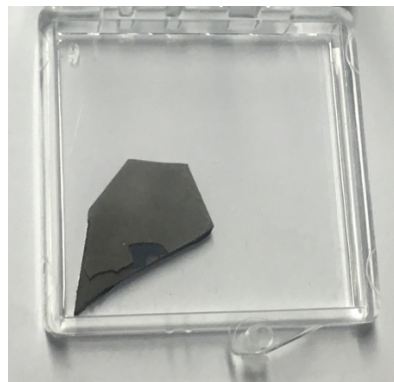

Figure 21. Sample GaNAl_1.5.2 with 1.5 nm Al interlayer delaminated and cracked at the edge of the sample.

3.2.1.1 SEM Imaging Characterization

The second sample with a 1.5 nm Al interlayer GaNAl_1.5.2 did not show signs of delamination after both visual inspection with the naked-eye and SEM imaging. Uniform, continuous diamond deposition was observed across the whole sample area. Similarly to Figure 16, no gaps were visible on the diamond film and diamond grains of mixed sizes were identified due to the mixed seeding method. The SEM image (Figure 22) confirmed that the presence of an Al interlayer does not negatively interfere with CVD diamond deposition or impact the extent of diamond coverage of the sample.
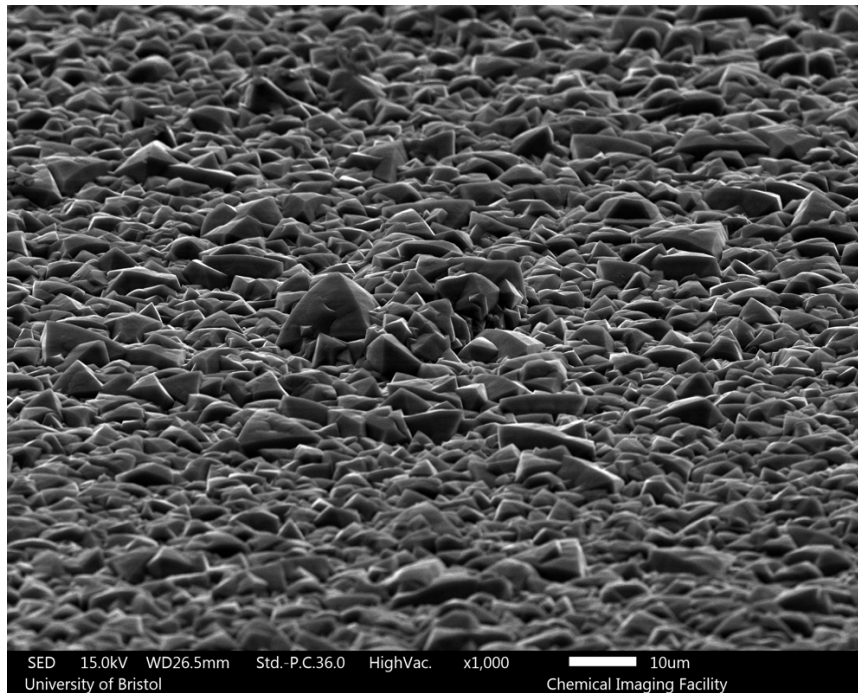
Figure 22. SEM Image at 75° angle and 1000 × magnification of delaminated diamond film surface on GaNAl_1.5.2 with 1.5 nm Al interlayer.

3.2.2.2 XRT Imaging Characterization
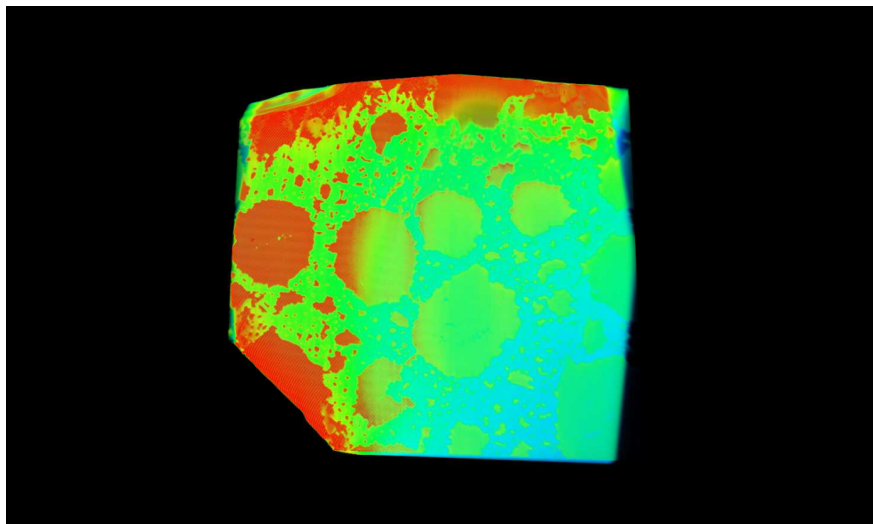
Figure 23. Top down view of XRT 3-D model of sample GaNAl_1.5.2 displaying a green Si layer, a red GaN layer and a light blue diamond layer.

The 3-D model produced by XRT viewed from above provided valuable insight on the surface quality of the GaN and diamond layers post CVD diamond deposition. The 1.5 nm Al interlayer cannot be viewed by XRT as it is of very low thickness. The GaN layer has decomposed into Ga metal, identified as a webbing pattern of red Ga droplets in Figure 23 and N_2 gas. The GaN decomposition can be rationalized as H etching, which destroys the

GaN surface, resulting in gaps and decomposition. Also, GaN reacting with the 1.5 nm Al interlayer to form aluminium nitride leads to the decomposition of GaN. The contouring and colouring selected in the XRT 3-D model (Figure 23) highlights the Si, GaN and diamond layer and confirms that the 1.5 nm layer was not effective in increasing the adhesion between the constituent layers and permitting the deposition of a diamond layer without disrupting the surface and quality of the GaN layer. As mentioned previously, the second sample GaNAl_1.5.1 delaminated on the edge.
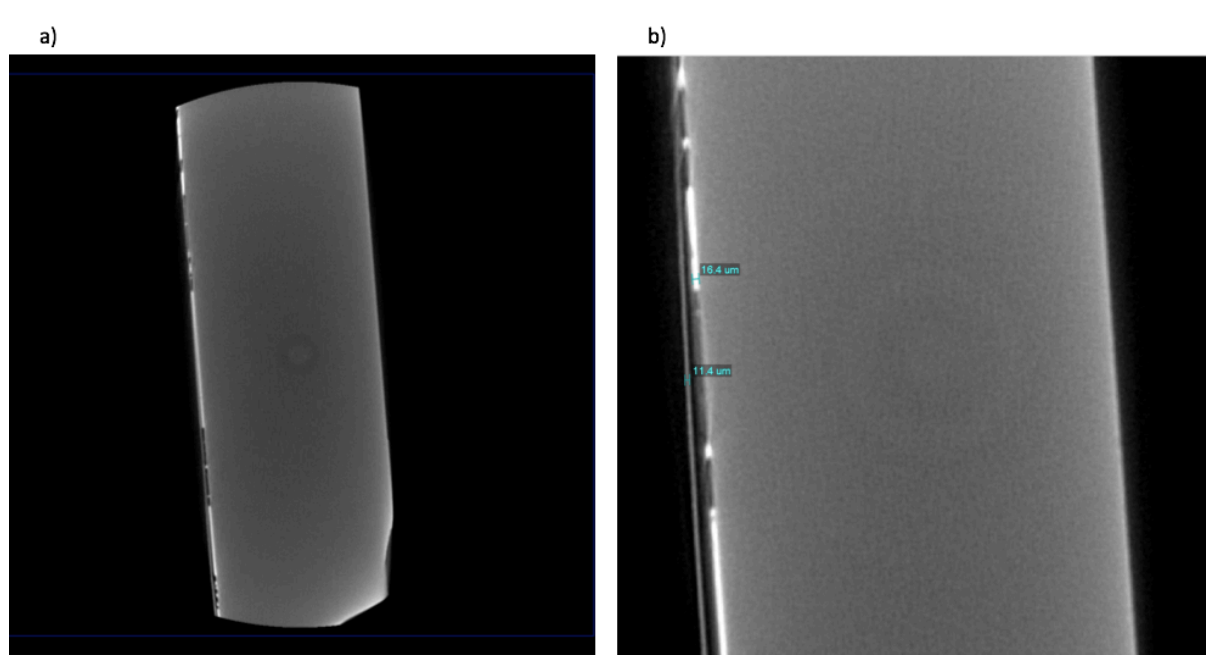

Figure 24. a) XRT image of side-view of GaNAl_1.5.2 sample b) Thickness measurements of GaN and diamond layers in GaNAl_1.5.2 sample based on XRT imaging.

H etching on the GaN layer has resulted in the decomposition of GaN on the surface, where Ga metal droplets are visible in Figure 23. The negative effect of H etching is also clearly illustrated in Figure 24 a), where ~ 3 large gaps and ~6 small gaps are present in the GaN layer coloured white. The GaN layer is discontinuous and damaged, however the diamond film is attached to the GaN and Al interlayer and has not delaminated. This observation was not expected as a diamond film bonded to a damaged GaN layer with large gaps was predicted to delaminate. The thickness of the GaN and diamond layer were measured as 16.4, 11.4 μm respectively, based on XRT imaging in Figure 24 b). XRT was used for thickness calculations of the diamond layer as thickness calculations based on SEM were not possible for sample GaNAl_1.5.2 as delamination of the diamond film was not observed.

It is important to note that measurements based on XRT imaging have significant errors associated and should be considered with caution. The expected thickness of the diamond

layer based on the typical rates of 1-5 µm h^{-1} after a 6-hour growth run was 6-30 µm, thus the growth rate of GaNAl_1.5.2 was ~2 µm h^{-1}, which is rational.
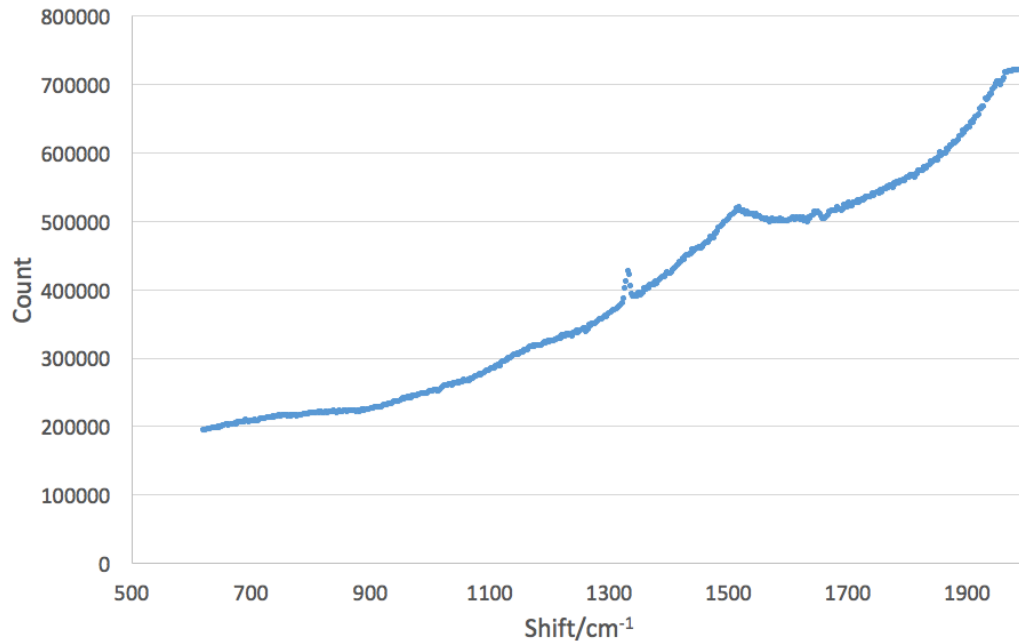
3.2.2.3 Raman Spectroscopy

Figure 25. Raman spectrum of diamond on GaNAl_1.5.2 with 1.5 nm Al interlayer after CVD diamond growth run obtained using a laser at 514 nm wavelength.

The sharp peak at 1332 cm^{-1} seen in Figure 25 due to sp^3 C-C bonds confirmed the presence of diamond on the GaNAl_1.5.2 sample and the broader, weaker peak at ~ 1580 cm^{-1} accounts for the graphitic sp^2 carbon also deposited during CVD and the sp^2 C-C bonds in aluminium carbide present from the reaction of Al and diamond. The FWHM was also determined using a 100% Gaussian fit on the 1332 cm^{-1} diamond peak in Figure 25. The FWHM for the GaNAl_1.5.2 sample was 8.99 cm^{-1}, which is lower in value than the FWHM for the GaN control sample. This suggests the presence of less strain in the GaNAl_1.5.2 sample upon incorporation of an interlayer. The aluminium carbide formed, bonding the GaN and diamond layer at the interface, reduces the stress in the GaNAl_1.5.2 sample [54] [55]. The Raman spectrum on a sample with an Al interlayer confirmed the diamond growth expected and permitted the continuation of this investigation using Al as an interlayer.

3.2.2 CVD Diamond Growth on GaN with 5.5 nm Al interlayer

Following the delamination of one of the samples coated with a thin Al layer of 1.5 nm thickness, the investigation continued with CVD diamond growth on two samples with a thicker 5.5 nm Al layer. By visible inspection, sample GaNAl_5.5.1 had a smooth coating of diamond on the surface with no signs of delamination or cracks. The 5.5 nm Al thickness was promising as it was hypothesized that it is of high enough thickness to deposit a continuous uniform layer of Al atoms and simultaneously does not greatly decrease thermal conductivity k at the interface. At 5.5 nm Al thickness the formation of aluminium carbide bonded the GaN and diamond layers strongly. However, the second sample GaNAl_5.5.2 showed great signs of delamination and had multiple cracks in the middle of the sample surface.

3.2.2.1 SEM Imaging Characterization

Figure 26. SEM Image at 75° angle and 500 × magnification of delaminated diamond film on GaNAl_5.5.2 with 5.5 nm Al interlayer. Along the middle of the sample the diamond film has cracked and a part of the diamond film is elevated from the deposited diamond layer on GaN.

Imaging of one of the delaminated areas of sample GaNAl_5.5.2 focused on the largest crack that runs through the middle of the sample. The crack in Figure 26 was estimated to have length~200 μm and was visible by the naked eye after the diamond growth run and thus was not caused by handling of the sample post growth. Diamond grains fully covered the entire surface area without any gaps detected.
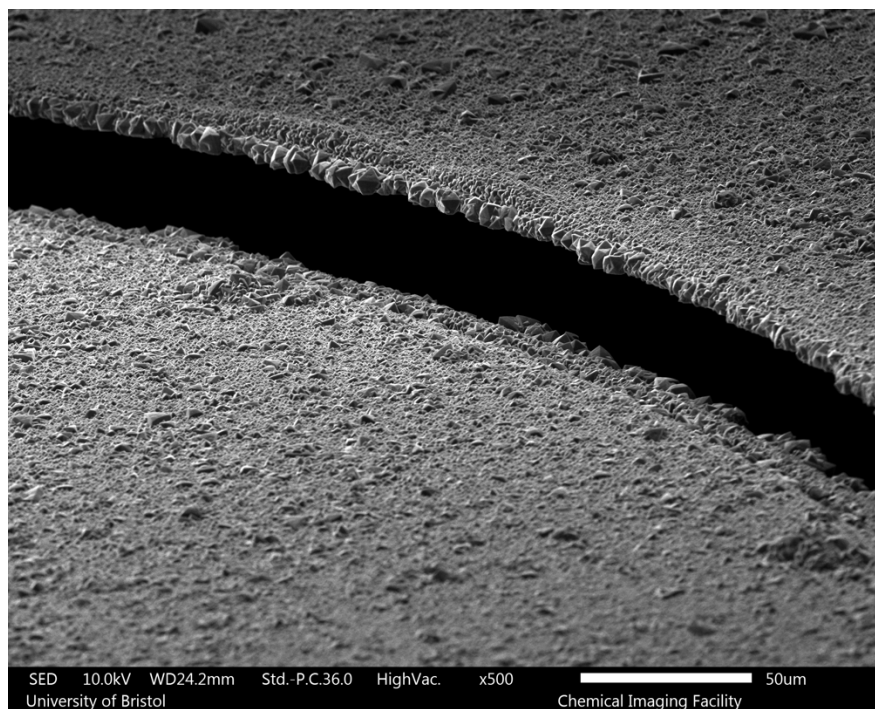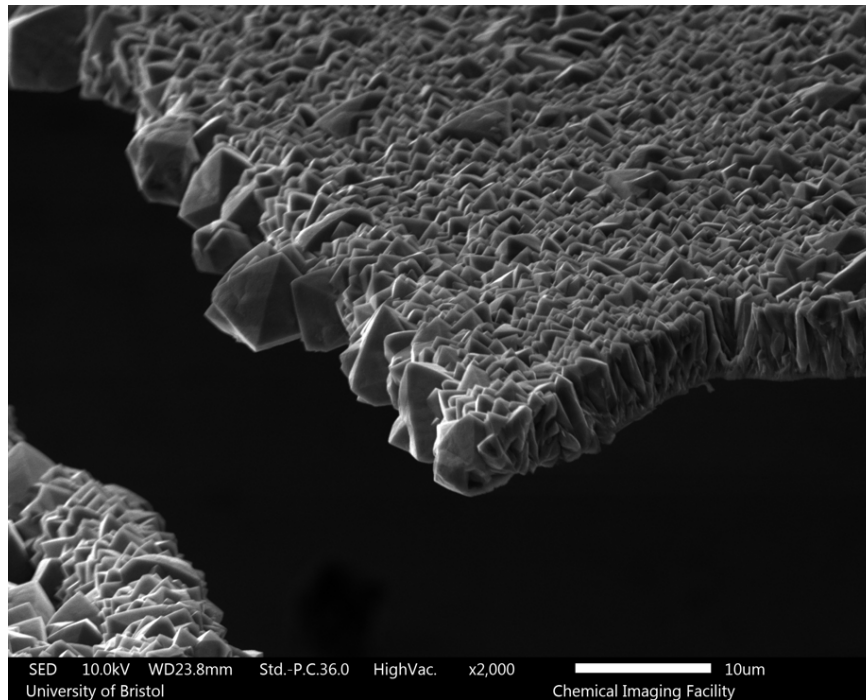
Figure 27. SEM Image at 75° angle and 2000 × magnification of delaminated diamond film on GaNAl_5.5.2 with 5.5 nm Al interlayer.

An interesting observation was made by focusing on the edge of the delaminated part of the diamond film at 2000 × magnification (Figure 27). Large fully formed diamond grains were identified on the edge of the delaminated diamond film indicating that the delamination occurred during the CVD diamond growth run and not during cooling. Diamond films that delaminate during cooling do not show large diamond grains on the edges of the surface (Figure 18). It can be inferred that the tensile interfacial stress during the growth at elevated temperature caused delamination of the diamond film at an earlier stage than cooling. Alternatively, a large temperature fluctuation during the growth run, where the sample was heating and cooling may have caused the delamination due to large interfacial stress.

It is hypothesized that a small percentage of the 5.5 nm Al interlayer reacted to form aluminium carbide. The Al that was not converted into aluminium carbide significantly increasing the thermal expansion coefficient mismatch between GaN, diamond and Al, as Al has a thermal expansion coefficient of 24.4×10^{-6} K^{-1}. This large mismatch contributed to high interfacial stress and accounts for the rapid delamination of the diamond film during the growth run seen in Figure 26, before the cooling phase.

The average thickness of the diamond layer based on SEM imaging, considering the 75° angle of the GaNAl_5.5.2 sample, was estimated ~ 6.6 μm by taking measurements at different parts of the layer in Figure 26. Overall, the interface formed including the 5.5 nm Al layer was weak and did not assist the close-packing of the diamond and GaN surfaces.
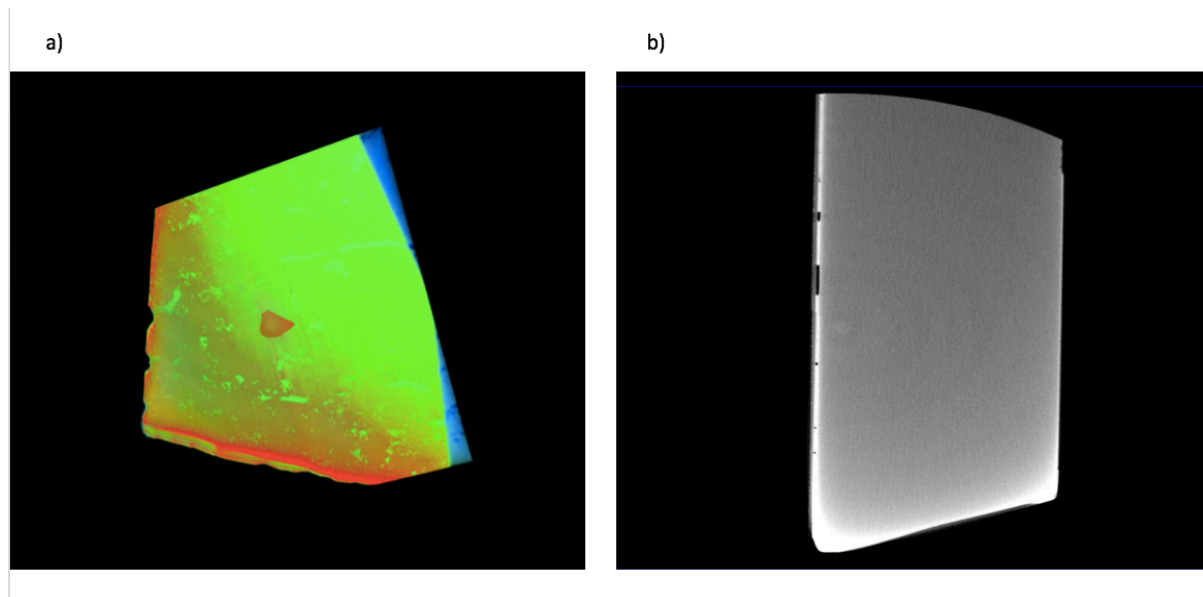
3.2.2.2 XRT Imaging Characterization

Figure 28. a) Top-down XRT 3-D model of GaNAl_5.5.1 sample displaying a green Si layer, a red GaN layer and a light blue diamond layer b) XRT side-view image of GaNAl_5.5.1 sample.

The incorporation of a 5.5 nm Al interlayer resulted in the deposition of a uniform and continuous diamond layer that did not delaminate as seen in light blue colour attached to the red GaN layer beneath (Figure 28 a)). The red GaN layer has not decomposed and is to great extent continuous and uniform with some parts of the surface etched away by H, making the green Si surface underneath it visible (Figure 28 a)). GaNAl_5.5.1 was vastly different to Figure 22, where sample GaNAl_1.5.2 contained a damaged and decomposed GaN layer after CVD diamond deposition with Ga droplets clearly visible in the XRT 3-D model. Three significant gaps in the GaN layer were identified in Figure 28 b), a result of H etching during CVD diamond growth. The thicker 5.5 nm Al interlayer, compared to the 1.5 nm Al interlayer previously explored, significantly coated and protected the GaN layer from severe H etching and decomposition. It is hypothesized that the formation of aluminium carbide, from the reaction of the 5.5 nm Al layer with diamond, promotes the adhesion between GaN and diamond layers, also resulting in a GaN layer that is less exposed and susceptible to H etching. As a result, less gaps in the GaN layer were identified in the sample with a 5.5 nm layer in Figure 28 b) compared to the ~ 9 gaps shown in the sample with a 1.5 nm Al layer coloured white in Figure 24 b).
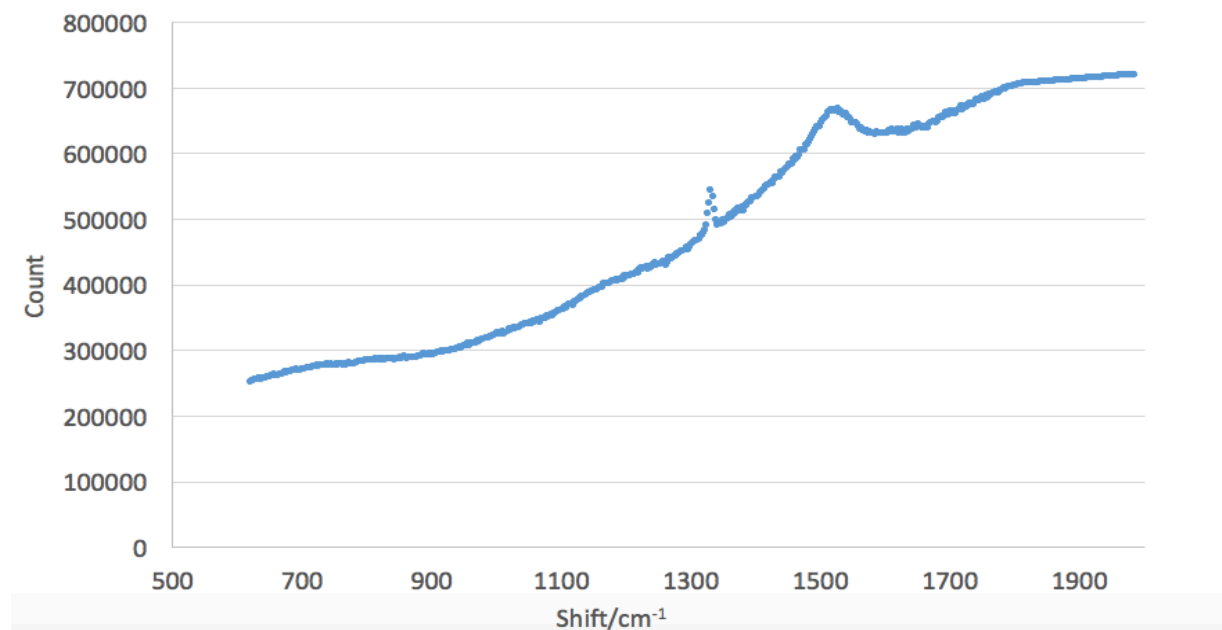
3.2.2.3 Raman Spectroscopy

Figure 29. Raman spectrum of diamond on GaNAl_5.5.1 with 5.5 nm Al interlayer after CVD diamond growth run obtained using a laser at 514 nm wavelength.

As in Figure 25 the sharp peak at 1332 cm^{-1} in Figure 28 confirmed the presence of diamond on the GaNAl_5.5.1 sample and the broader, weaker peak at $\sim$ 1580 cm^{-1} accounts for the aluminium carbide formed and graphitic carbon also deposited during CVD. The FWHM was also determined using a 100% Gaussian fit on the 1332 cm^{-1} diamond peak in Figure 29. The FWHM for the GaNAl_5.5.1 sample was 8.91 cm^{-1}, which is lower in value than the FWHM for the GaN_1.5.2 sample. The lower FWHM for sample GaNAl_5.5.1 suggested the presence of less strain in the sample upon incorporation of a 5.5 nm Al interlayer of greater thickness compared to the 1.5 nm Al interlayer. It is hypothesized that more aluminium carbide is formed upon incorporation of the thicker 5.5 nm Al interlayer compared to the 1.5 nm Al interlayer. The aluminium carbide bonded the GaN and diamond layer at the interface, reducing the stress in the GaNAl_5.5.1 sample [54] [55].

In overview, the SEM imaging suggested that the both the 1.5 and 5.5 nm Al interlayer are too thin to form a strong chemically bonded interface containing aluminium carbide and overall result in delamination. The investigation proceeded with the incorporation of an Al interlayer of greater thickness.

Elena C. Persaud

3.2.4 CVD Diamond Growth on GaN with 20.0 nm Al interlayer

The severe delamination and cracks on the GaNAl_5.5.1 sample with a 5.5 nm Al interlayer prompted the incorporation of an Al interlayer of much greater thickness. A 20.0 nm Al interlayer coated samples GaNAl_20.0.1 and GaNAl_20.0.2.

3.2.4.1 SEM Imaging Characterization
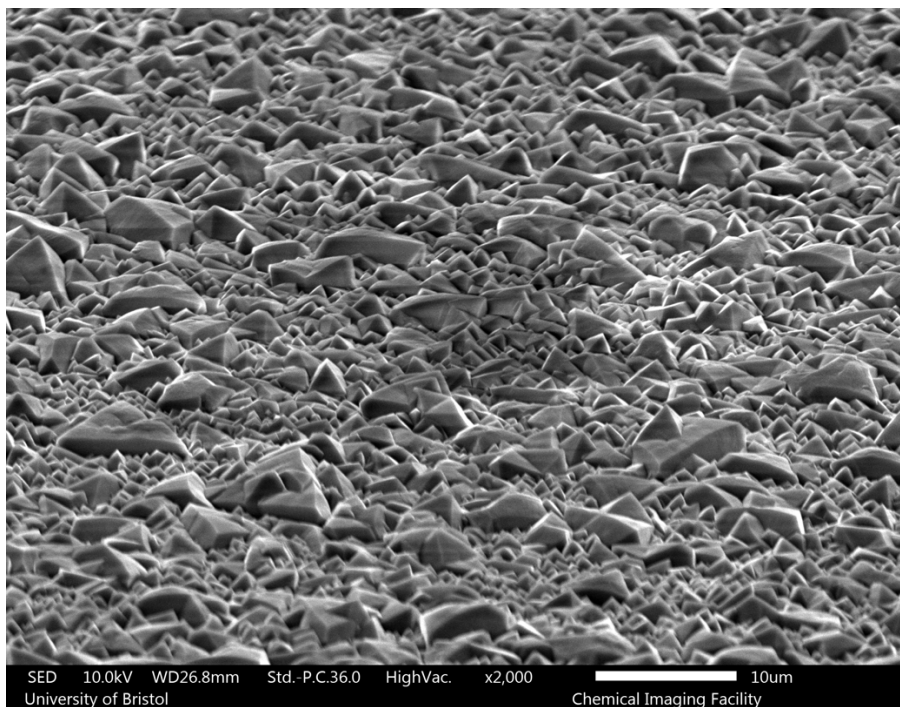
Figure 30. SEM Image at 75° angle and 2000 × magnification of diamond film surface on GaNAl_20.0.1 with 20.0 nm Al interlayer.

The sample surface of the entire sample GaNAl_20.0.1 was inspected by SEM shown in Figure 30. The extent of coverage of the sample surface with closely-packed diamond grains was ~100%, with no visible gaps or exposed Al surface, similar, to Figure 16 and Figure 22. A part of the sample surface was magnified 2000 × (Figure 30), where diamond grains of varying sizes were formed from the growth of micro- and nanodiamond seeds deposited during mixed seeding.

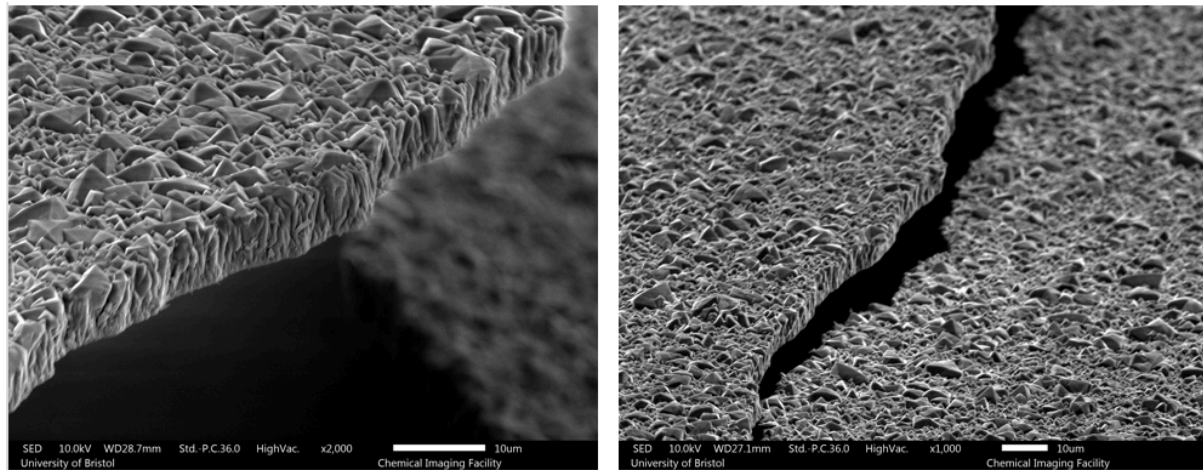Figure 31. (a) SEM Image at 75° angle and 2000 × magnification focusing on the edge of delaminated diamond film on GaNAl_20.0.1 with 20.0 nm Al interlayer b) SEM Image at 75° angle and 1000 × magnification of delaminate diamond film surface on GaNAl_20.0.1 with 20.0 nm Al interlayer.

No cracks or signs of delamination were visible on samples GaNAl_20.0.1 and GaNAl_20.0.2 after the CVD diamond growth run was terminated. However, the delamination apparent in both SEM images (Figure 31) was caused by mounting sample GaNAl_20.0.1 on the substrate holder in the SEM apparatus. The samples in this investigation were very sensitive to any physical handling and can delaminate and crack spontaneously. Delamination observed during CVD growth in Figure 26 resulted in the delaminated diamond film being ∼ 30 μm above the sample surface. Delamination during cooling in sample (Figure 17) resulted in the delaminated diamond film being ∼70 μm above the sample surface. In comparison, sample GaNAl_20.0.1 in Figure 31 b) resulted in the delaminated diamond film being 7 μm above the sample surface confirming that delamination occurred post-growth and post-cooling. No large, fully formed diamond grains were identified in Figure 31 a) focusing on the edge of the delaminated diamond film. For this reason, the delamination did not occur during the CVD growth run. In overview, both samples containing a 20.0 nm Al interlayer did not delaminate and promoted the close-packing of the diamond and GaN by forming a strong and effective interface. It is hypothesized that the 20.0 nm Al interlayer was of the substantial thickness that is required to form aluminium carbide and chemically bond the Al and diamond layers to improve adhesion. Al has a thermal expansion coefficient of $24.4 \times 10^{-6} \text{ K}^{-1}$, and has a great thermal expansion coefficient mismatch with GaN and diamond as mentioned in page 32. Thus, the conversion of a large percentage of Al into aluminium carbide greatly reduces the probability of delamination by reducing this large mismatch between the constituent layers.

The average thickness of the diamond layer based on SEM imaging considering the 75° angle of the GaNAl_20.0.1 sample was estimated ~ 9.0 μm by taking measurements at different parts of the layer in Figure 31 a).
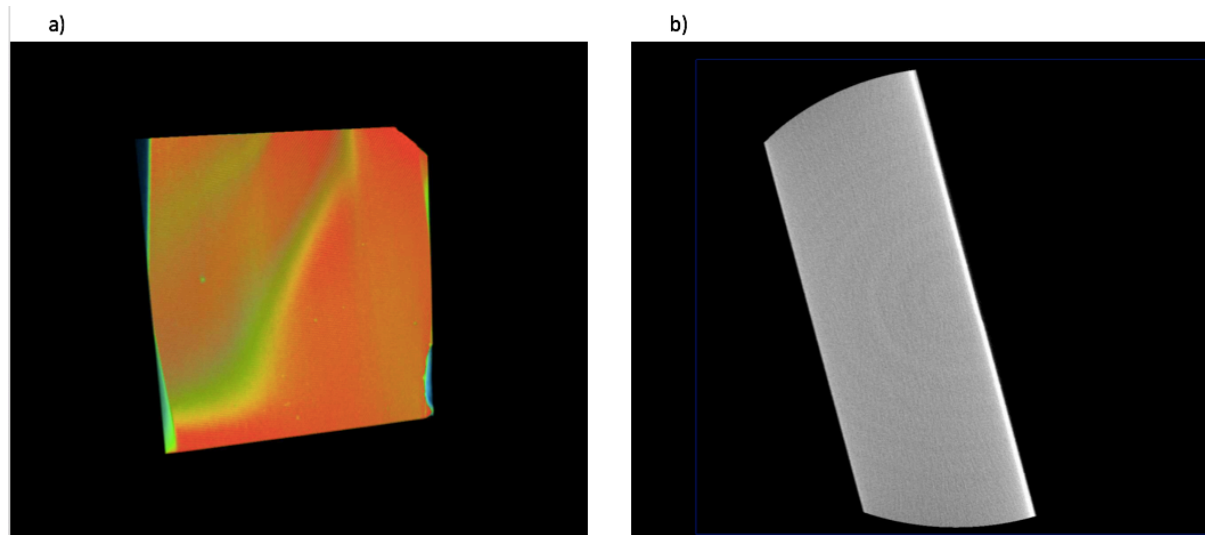
3.2.4.2 XRT Imaging Characterization

Figure 32. a) Top-down XRT 3-D model of GaNAl_20.0.2 sample displaying a green Si layer, a red GaN layer and a light blue diamond layer b) XRT side-view image of GaNAl_20.0.2 sample.

The use of a 20 nm Al interlayer incorporated in sample GaNAl_20.0.2 greatly contributed to the strong adhesion between the GaN and diamond layers. As illustrated in Figure 32 b) the diamond film has not delaminated and is attached to the GaN layer coloured white. It is hypothesized that a high percentage of the thick 20.0 nm Al interlayer reacted with diamond to form aluminium carbide that chemically bonds the GaN and diamond. As seen in Figure 32 b) the Si, GaN and diamond layers are closely packed leaving no gaps in between layers. The aluminium carbide formed effectively protects the GaN layer from H etching, which would otherwise create visible gaps in the GaN layer, similar to Figure 24 b). H etching also results in GaN decomposition forming Ga droplets seen in Figure 23. In contrast, the red GaN layer has remained smooth and very continuous after CVD diamond deposition and has not decomposed at any parts of the layer (Figure 32 a)). H etching has not affected the GaN layer, which as seen in Figure 32 b) has no gaps and is fully attached at all parts to the diamond film. The second sample with a 20.0 nm Al interlayer GaNAl_20.0.2 characterized by SEM also resulted in a CVD deposition of high quality, where the sample surface was uniformly covered with diamond grains and no gaps were identified as shown in Figure 30. The delamination in GaNAl_20.0.2 as mentioned previously was caused by loading the sample

onto the SEM substrate holder. The 20.0 nm Al interlayer was ~four times thicker than the 5.5 nm Al interlayer explored previously and was considered an interlayer thickness of more appropriate thickness compared to the 1.5 and 5.5 nm interlayers used previously.
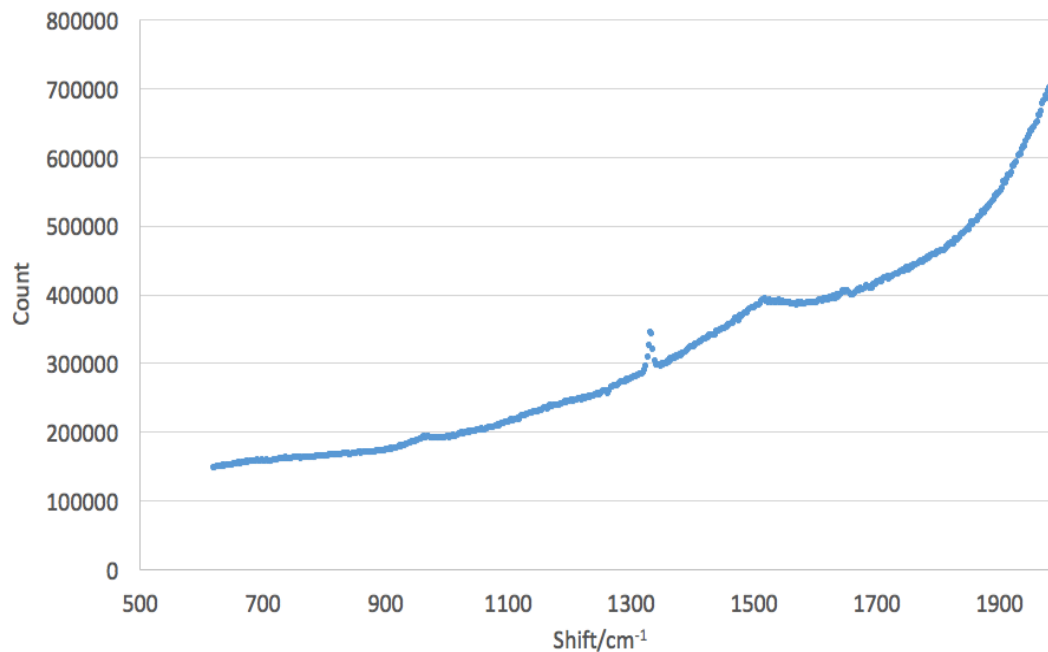
3.2.4.3 Raman Spectroscopy

Figure 33. Raman spectrum of diamond on GaNAl_20.0.1 with 20.0 nm Al interlayer after CVD diamond growth run obtained using a laser at 514 nm wavelength.

Similar to the previously discussed Raman spectra in Figures 25 and 29, the sharp peak at 1332 cm^{-1} in Figure 33 confirmed the presence of diamond on the GaNAl_20.0.1 sample and the broader, weaker peak at ~ 1580 cm^{-1} accounts for the aluminium carbide formed and graphitic carbon also deposited during CVD. The FWHM was determined using a 100% Gaussian fit on the 1332 cm^{-1} diamond peak in Figure 33. The FWHM for the GaNAl_20.0.1 sample was 7.88 cm^{-1}, which is lower in value than the FWHM for the GaN_5.5.1 sample and GaN_1.5.2. The lower FWHM for sample GaNAl_20.0.1 suggested the presence of less strain in the sample upon incorporation of a 20.0 nm Al interlayer of greater thickness compared to the 5.5 nm Al interlayer. It is hypothesized that more aluminium carbide was formed upon incorporation of the thicker 20.0 nm Al interlayer compared to the 1.5 and 5.5 nm Al interlayers, bonding the GaN and diamond layer at the interface, reducing the stress in the GaNAl_20.0.1 sample [54] [55].

3.2.5 CVD Diamond Growth on GaN with 40.3 nm Al interlayer

The CVD diamond growth run on the two duplicate samples containing a 20.0 nm Al interlayer resulted in the deposition of a continuous diamond layer that did not crack or delaminate during the growth or the cooling phase. To add to that, the GaN layer did not decompose and was not negatively affected by H etching. The last sample of this investigation, GaNAl_40.3.1 was coated with a thick 40.3 nm Al interlayer. Based on the outcome of the samples containing the 20.0 nm Al interlayer it was hypothesized that sample GaNAl_40.3.1 will not delaminate, as it contains an interlayer of comparable thickness.

3.2.5.1 SEM Imaging Characterization

Figure 34. SEM Image at 75° angle and 500 × magnification of diamond film surface and edge of GaNAl_40.3.1 with 40.3 nm Al interlayer.

The 6-hour CVD diamond growth run produced a continuous diamond film in Figure 34, where the sample surface and edge were fully covered with diamond grains. There were no signs of delamination present or cracks in sample GaNAl_40.3.1, which confirmed the hypothesis formed after the successful outcome of growth runs on samples GaNAl_20.0.1 and GaNAl_20.0.2. The thick 40.3 nm Al interlayer has reacted to a great extent with the diamond layer to form aluminium carbide, bonding the diamond and GaN layers strongly.
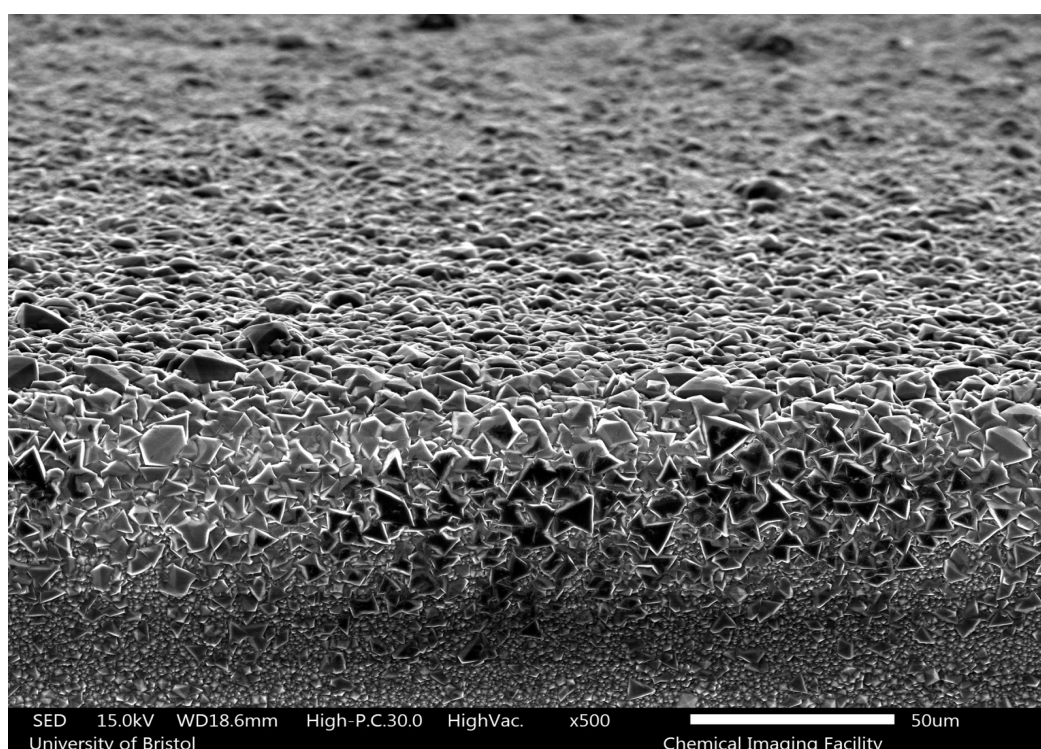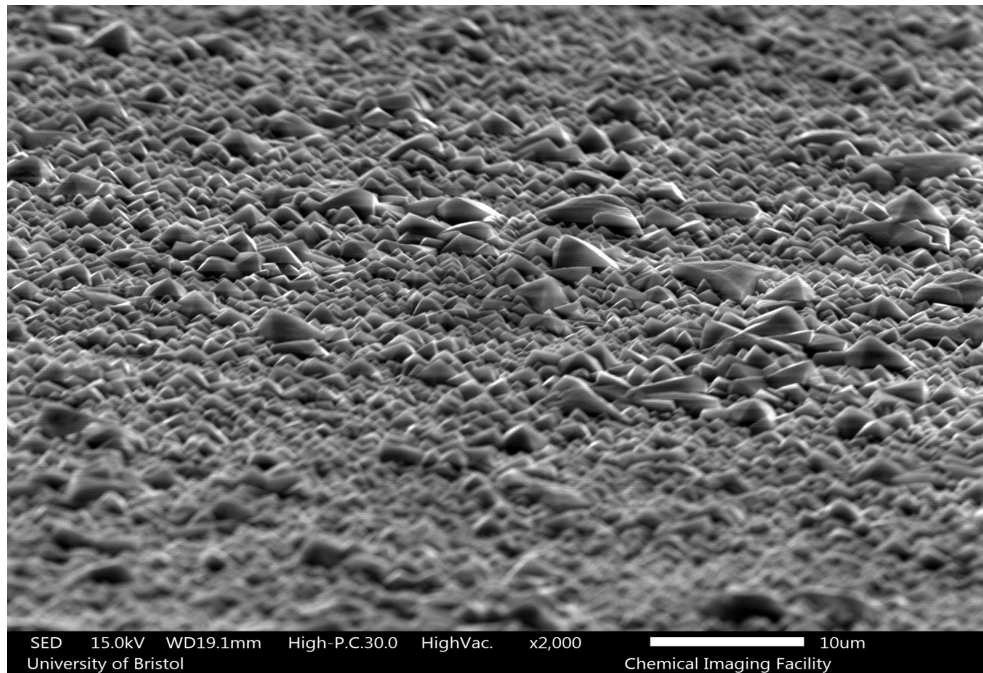
Figure 35. SEM Image at 75° angle and 2000× magnification of diamond film surface and edge of GaNAl_40.3.1 with 40.3 nm Al interlayer.

No gaps in the diamond film were identified in Figure 35, as the nanodiamonds deposited during mixed seeding have covered the gaps in between the larger in size microdiamonds, similar to Figure 30. Due to a limited amount of samples that could be characterized by XRT, the sample GaNAl_40.3.1 could not be characterized for this investigation. Viewing the sample through XRT would illustrate the quality of the GaN layer post-growth and the extent of H etching during the run.

3.2.5.2 Raman Spectroscopy

Figure 34. Raman spectrum of diamond on GaNAl_40.3.1 with 40.3 nm Al interlayer after CVD diamond growth run obtained using a laser at 514 nm wavelength.

Similar to the previously discussed Raman spectra in Figures 29 and 33, the sharp peak at 1332 cm^{-1} in Figure 34 confirmed the presence of diamond on the GaNAl_40.3.1 sample and the broader, weaker peak at ~ 1580 cm^{-1} accounts for the aluminium carbide form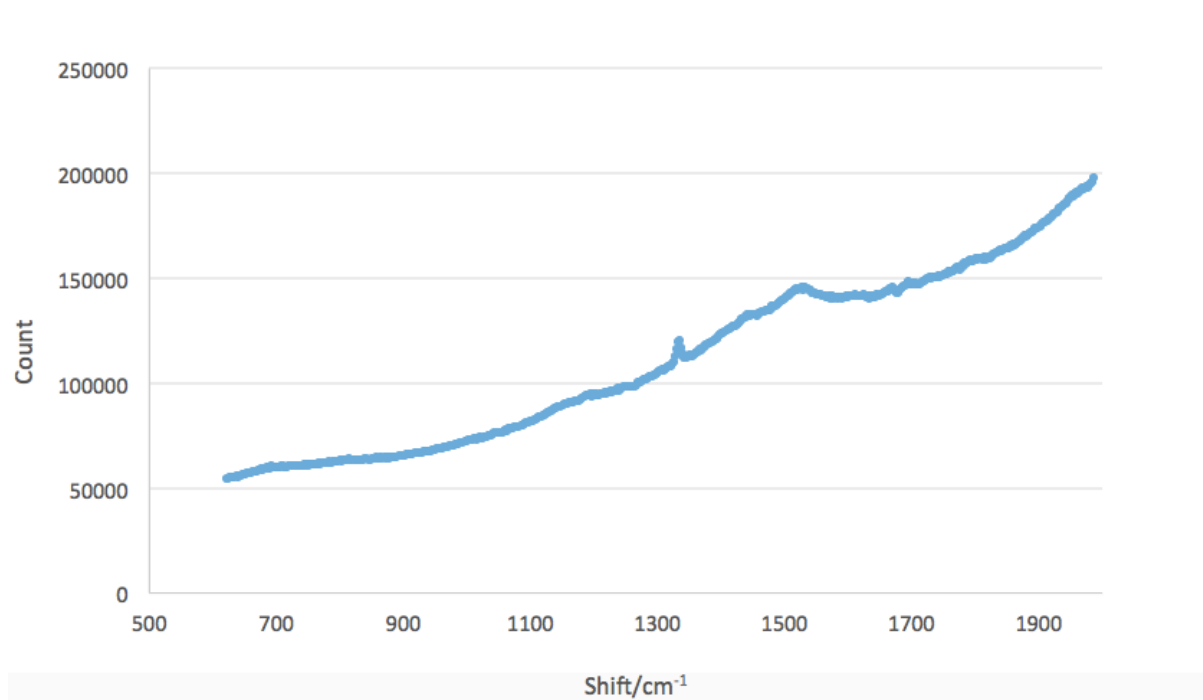ed and graphitic carbon also deposited during CVD. The FWHM was also determined using a 100% Gaussian fit on the 1332 cm^{-1} diamond peak in Figure 34. The FWHM for the GaNAl_40.3.1 sample was 7.80 cm^{-1}, which is slightly lower in value than the FWHM for the GaN_5.5.1 sample and GaN_20.0.1. The lower FWHM for sample GaNAl_40.3.1 suggested the presence of relatively less strain in the sample upon incorporation of a 40.3 nm Al interlayer of greater thickness compared to the 20.0 nm Al interlayer. It is hypothesized that more aluminium carbide was formed upon incorporation of the thicker 40.3 nm Al interlayer compared to the 1.5, 5.5 and 20.0 nm Al interlayers, bonding the GaN and diamond layer at the interface, reducing the stress in the GaNAl_40.3.1 sample [54] [55].

Conclusion

The experimental section of this thesis explored the incorporation of an interlayer between the GaN and diamond layers, in order to improve the interfacial adhesion quality and prevent delamination of the diamond layer. Diamond was successfully deposited on a seeded GaN and Al surface by 6-hour CVD diamond growth runs. The Raman spectra of the samples produced confirmed the presence of sp^3 diamond, along with graphitic sp^2 carbon that is present in aluminium carbide formed at the interface. Varying the thickness of the Al interfacial layer incorporated affected the adhesion quality of the diamond layer on the GaN layer. One of the 2 samples containing a 1.5 nm Al interlayer cracked and delaminated during cooling after CVD deposition, as illustrated by SEM imaging. XRT imaging displayed the decomposition of GaN into visible Ga droplets and the formation of voids in the GaN layer by H etching. One of the 2 samples with a 5.5 nm Al interlayer cracked in the middle of the sample and delaminated during CVD deposition, displayed by SEM imaging. XRT imaging illustrated the deposition of a relatively continuous diamond layer, where GaN did not decompose. Also, the voids formed in the GaN layer by H etching were significantly less compared to the H etching observed in the sample with the 1.5 nm Al interlayer. It was hypothesized that as the Al interlayer thickness increases, a greater proportion of Al reacts with diamond to form aluminium carbide, which chemically strengthens the interface and allows the GaN and diamond layer to chemically bond. The aluminium carbide relieved interfacial stress and protected the GaN layer from etching. CVD diamond growth on both samples containing a 20.0 nm Al interlayer resulted in the deposition of a smooth, continuous diamond layer without any cracks and no signs of delamination after the run. The GaN layer did not present any gaps as seen in the XRT images, indicating that H etching was limited during the run. The GaN layer was continuous and had not decomposed during the CVD diamond growth run. Similarly, the sample containing a 40.3 nm Al interlayer did not delaminate and facilitated the deposition of a continuous layer of diamond that covered the GaN surface fully. It was inferred that there was significant reaction of Al and diamond to form aluminium carbide in the samples containing the two thickest layers explored in this investigation of 20.0 and 40.3 nm. This magnitude of thicknesses produced an interface consisting of aluminium carbide that protected GaN from H etching and chemically bonded the GaN and diamond layers. However, it is important to note that no solid conclusions can be made without testing the CVD diamond growth on a larger number of duplicate samples containing a 20.0 and 40.3 nm Al interlayer that were shown to be successful in this investigation. To eliminate the possibility that the outcome of the diamond deposition on

these samples was random, future research should repeat the diamond growth on duplicate samples.

On the whole, the incorporation of an Al interlayer contributed to improving the adhesion quality at the interface as 5 of the 7 samples produced containing an Al interlayer did not delaminate, compared to the GaN control sample without an interlayer that did delaminate and crack. The following part of this thesis includes improvements that could be made in this investigation regarding the deposition of diamond-on-GaN for thermal management of high-power electronic devices and recommendations for future research on this topic.

Future Work

There is a number of suggestions and amendments regarding the future continuation of this investigation that should be highlighted. Initially, a larger number of duplicate samples should be produced for every Al interlayer thickness investigated in order to make the observations made more reliable. It is then possible to confirm that the delamination or adhesion in the wafer exists due to the change in the variable factor, the Al interlayer thickness, and not due to various other uncontrolled or random factors. Time constraints limited the number of sample duplicates produced to a maximum of two duplicates per different Al interlayer thickness.

Performing CVD diamond growth runs of a longer duration would result in the deposition of a diamond layer of greater thickness suitable to the typical thickness of diamond films incorporated currently in GaN-based High-Electron-Mobility Transistors.

This investigation originally included the diamond growth on samples incorporating titanium interlayers of varying thickness. Unfortunately, the microwave plasma-enhanced CVD reactor broke down during the allocated laboratory part of this investigation, and thus no data was collected regarding samples with a Ti interlayer. Titanium has a very high melting point of 1668 °C, compared to Al and will not melt and decompose during a growth run [60]. Al has a melting point of 660 °C and is susceptible to melting during diamond growth runs were temperatures of 700 ± 40 °C are reached [60]. Ti has a thermal expansion coefficient of 7.14×10^{-6} K^{-1} [58], which is closer than Al to the respective GaN value of 5.6×10^{-6} K^{-1} and diamond value 1×10^{-6} K^{-1}. The lower thermal expansion coefficient mismatch between Ti, GaN and diamond results in lower interfacial stress and greater adhesion between the layers. Ti reacts with diamond forming titanium carbide, which is a very hard material that forms a stronger lattice than aluminium carbide and is predicted to chemically bond the diamond and GaN layers together, strongly. Another interlayer that could be investigated is aluminium nitride that has a hexagonal crystal structure similar to GaN and a thermal expansion coefficient of 4.8×10^{-6} K^{-1} which is close to the GaN value of 5.6×10^{-6} K^{-1} and diamond value 1×10^{-6} K^{-1} [9] [8] [59]. However, at 700 °C oxidation at the AlN surface takes place which could have negative implications for the diamond layer deposited by CVD.

Thermal characterization of the samples in this investigation would provide data regarding the extent to which the rise in interlayer thickness lowers the thermal conductivity and increases thermal resistance (TBR_{eff}) at the diamond-on-GaN interface. However, access to

thermal characterization was not possible during this investigation, so this analysis could not be performed.

The 4 samples in this investigation that were not analysed by XRT should be characterized by this technique in the future, as decomposition of the GaN layer and the number of voids formed by H etching in the GaN layer can be seen clearly by XRT imaging. More specifically, a sample were the diamond film has not delaminated may still contain a decomposed GaN layer that includes voids and a damaged surface. It is critical to observe the outcome of the diamond deposition on the GaN layer in every sample in the investigation, in order to draw conclusions regarding the most effective thickness of Al interlayer included.

Future work could include the utilization of an alternative seeding method instead of mixed electrospray seeding. The zeta (ζ) potential seeding technique exploits the electric potential between the GaN layer and nanodiamond particles. This technique leads to an increase the coverage and density of diamond seeds situated on the GaN layer, limiting the surface area of exposed GaN which is otherwise susceptible to etching. Finally, a surface patterning technique could be used to treat the GaN surface. This technique etches suitable corrugations on the GaN surface, yielding an interface that physically locks the GaN and diamond layer together giving a greater ability to withstand the residual stresses. Therefore, an interfacial layer is not required, which as a result does not compromise the interfacial thermal conductivity k and thermal resistance (TBR_{eff}) at the diamond-on-GaN interface.

Elena C. Persaud

References

[1] S. J. Pearton, C. R. Abernathy, M.E. Overberg, G. T. Thaler, A. H. Onstine, B. P. Gila, F. Ren, B. Lou, J. Kim, *Materials Today*, 2002, **5**, 24-31

[2] University of Bristol, http://www.chm.bris.ac.uk/motm/diamond/diamondh.htm, (accessed November 2018)

[3] Inflibnet Centre, http://shodhganga.inflibnet.ac.in/bitstream/10603/77200/8/08_chapter%201.pdf, (accessed November 2018)

[4] M. Seelmann-Eggebert, P. Meisen, F. Schaudel, P. Koidl, A. Vescan, H. Leier, *Diamond and Related Materials*, 2001, **10**, 744-749

[5] H. de Wit, *The Element Six CVD Diamond Handbook*, Element Six Technologies, Ascot, 2017

[6] I. Yonenaga, *Journal of Nitride Semiconductor Research,* 2002, **7,** 1

[7] A. Bundy, P. Bassett, W. A. Weathers, M. S. Hemley, R. J. Mao, H. K. Goncharov, *Carbon*, 1996, **34**, 141–153

[8] M. E. Levinshtein, S. L. Rumyantsev, M. S. Shur, *Properties of Advanced Semiconductor Materials GaN, AlN, InN, BN, SiC, SiGe*, John Wiley & Sons, Toronto, 2001

[9] F. Medjdoub, *Gallium Nitride (GaN) Physics, Devices and Technology*, CRC Press, Boca Raton, 2016

[10] V. I. Volga, L. M. Buchnev, N. V. Markelov, B.K Dymov**,** *Sint. Almazy***,** 1976, **3**, 9-11

[11] S. Lee, S. Y. Kwon, H. J. Ham, *Japanese Journal of Applied Physics*, 2011, **50**

[12] A. Motayed, A. V. Davydov, S. N. Mohammad, J. Melngailis, *Journal Of Applied Physics*, 2008,104

[13] University of Bristol, http://www.chm.bris.ac.uk/motm/diamond/diamondh.html, (accessed November 2018)

[14] University of Bristol, http://www.bris.ac.uk/Depts/Chemistry/MOTM/diamond/diamond.html, (accessed October 2018)

[15] P. W. May, C. A. Rego, N. M. Everitt, M. N. R. Ashfold, *Chemical Society Reviews*, 1994, 22

[16] J. J. Gracio, Q. H. Fan, J. C. Madaleno, *Journal of Physics D: Applied Physics*, 2010, **43**

[17] P.W. May, *Endeavour,* 1995, **19**, 102

[18] J. J. Gracio, Q. H. Fan, J. C. Madaleno, *Journal of Physics D: Applied Physics*, 2010, **43,** 6

Elena C. Persaud

[19] P. W. May, *Phil. Trans. R. Soc. Lond. A*, 2000**, 358**, 476-480

[20] T. Zhang, Y. Zou, *Coatings*, 2017, **7,** 3

[21] J. J. Gracio, Q. H. Fan, J. C. Madaleno, *Journal of Physics D: Applied Physics*, 2010, **43**, 13

[22] S. A. Chambers, *The Chemical Physics of Solid Surfaces*, Elsevier, 2001

[23] C. Kittel, *Introduction to Solid State Physics*, John Wiley & Sons, 1996

[24] D. L. Pierre, M. Bruno, F. Nestola, M. Prencipe, C. Manfredotti, *Molecular Physics*, 2014, **112**, 1030-1039

[25] H. Marchand, PhD Thesis, University of California, 2002

[26] G. Banflavi, *Cent. Eur. J. Chem*., 2012, **5**, 1676-1680

[27] Radboud University Nijmeden, http://www.vcbio.science.ru.nl/en/fesem/applets/diamond/, (accessed November 2018)

[28] T. Hanada, Advances in Materials Research, 2019, **12**

[29] Namlab, http://www.namlab.de/research/energy-efficiency-devices/gallium-nitride-based-device-technology, accessed October 2018)

[30] Efficient Power Conversion Corporation, https://epc-co.com/epc/GalliumNitride/WhatisGaN.aspx, (accessed October 2018)

[31] Business Wire, https://www.businesswire.com/news/home/20161025006596/en/Top-6-Vendors-Global-GaN-Devices-Market, (accessed October 2018)

[32] L. Yates, J. Anderson, X. Gu, C. Lee, T. Bai, M. Mecklenburg, T. Aoki, M. S. Goorsky, M. Kuball, E. L. Piner, S. L. Graham, *ACS Applied Materials & Interfaces,* **10,** 2018, 24302-24309

[33] University of Bristol, http://www.bristol.ac.uk/physics/news/2017/--ultra-high-power-gan-on-diamond-microwave-device-transforming-communication-an.html, (accessed October 2018)

[34] M. Seelmann-Eggebert, P. Meisen, F. Schaudel, P. Koidl, A. Vescan, H. Leier , *Diamond and Related Materials*, 2001, **10**, 744-749

[35] D. Liu, D. Francis, F. Faili, C. Middleton, J. Anaya, J. W. Pomeroy, D. J. Twitchen, M. Kuball, *Scripta Materalia*, 2017, **128,** 57-60

[36] P.W. May, H.Y. Tsai, W.N. Wang, J.A. Smith, *Diamond & Related Material,* 2006, **15**, 526-530

[37] P. A. Nistor, P.W. May, *J. Roy. Soc. Interface,* 2017, **14**, 4

[38] J. W. Pomeroy, R. B. Simon, H. Sun, D. Francis, F. Faili, D. J. Twitchen, M. Kuball, *IEEE Electron Device Letters*, 2014, **35**, 1007-1009

[39] T. Bai, M. S. Goorsky, Y. Wang, T.I. Feygelson, M. J. Tadjer, K. D. Hobart, S. Graham, *ECS Transactions*, 2018, **86**, 9-14

[40] S. Mandal, Evan L. H. Thomas, C. Middleton, L. Gines, J. Griffiths, M. Kappers,
R. Oliver, D. J. Wallis, L. E. Goff, S. A. Lynch, M. Kuball, O. A. Williams, *ACS Omega*, 2017,7276-7279

[41] O. J. L. Fox, J. O. P. Holloway, G. M. Fuge, P. W. May, M. N. R. Ashfold, *Mater. Res. Soc.*, 2010, **1203**, 1

[42] P. W. May, A. Piracha, Unpublished, 2018

[43] E. C. Persaud, University of Bristol, 2018

[44] Y. Chakk, R. Brener, A. Hoffman, *Appl. Phys. Lett.*, 1995, **66**, 2819

[45] M. Varga, T. Izak, A. Kromka, M. Vesely, K. Hruska, M. Michalka, *Cent. Eur. J. Physics*, 2012, **10,** 218-224

[46] L. Qinghuang*, Physical Properties of Polymers Handbook*, 2007, 941-942

[47] T. Sreenidhi, K. Baskar, A. DasGupta, N. DasGupta, *IOP Publishing*, 2008, 399-402

[48] J. Lee, K. Chang, I. Lee, S. Park, *J. Electrochem. Soc.,* 2000, **147**, 1859-1860

[49] Adapted from: University of Washington, https://users.wfu.edu/ucerkb/Nan242/L15-Photolithography.pdf, (accessed December 2018)

[50] X. Wei, PhD Thesis, Georgia Institute of Technology, 2004

[51] S. V. Garimella, T. Harrichian*, Encyclopedia of Thermal Packaging*, World Scientific Publishing Company, 2013

[52] University of Bristol, http://www.chm.bris.ac.uk/pt/diamond/seeding.html, (accessed November 2018)

[53] Springer, https://link.springer.com/content/pdf/bbm%3A978-1-4757-4751-5%2F1.pdf, (accessed November 2018)

[54] W. L. Wang, M. C. Polo, G. Sanchez, J. Cifre, J. Esteve, *Journal of Applied Physics*, 1996, **80,** 1846

[55] M. Vashista, S. Paul, Philosophical Magazine, 2012, **92**

[56] National Institute of Standards Technology, https://nvlpubs.nist.gov/nistpubs/jres/048/jresv48n3p209_a1b.pdf, (accessed November 2018)

[57] D. K. Palchaev, Z. K. Murlieva, K. S. Palchaeva, Journal of Engineering Physics & Thermophysics, 1994, **66**, 661

[58] P.Hindert, *Part of Journal of Research of the National Bureau of Standards,* 1943, **30,** 103

[59] Azom, https://www.azom.com/properties.aspx?ArticleID=610, (accessed December 2018)

[60] D. R. Lide, *CRC Handbook of Chemistry and Physics 88th Edition*, CRC Press, 2007

[61] J. Dinley, L. Hawkins, G. Paterson, A. Ball, L. Sinclair, P.Sinnet-Jones, S. Lanham, *Journal of Microscopy*, 2010, **238**, 123-133